MethodsX 10 (2023) 102181

Contents lists available at ScienceDirect

MethodsX

journal homepage: www.elsevier.com/locate/mex

Many-objective meta-heuristic methods for solving constrained truss optimisation problems: A comparative analysis

Natee Panagant[a], Sumit Kumar[b], Ghanshyam G. Tejani[c,*], Nantiwat Pholdee[a], Sujin Bureerat[a]

[a] *Sustainable Infrastructure Research and Development Center, Department of Mechanical Engineering, Faculty of Engineering, Khon Kaen University, Khon Kaen 40002, Thailand*
[b] *Australian Maritime College, College of Sciences and Engineering, University of Tasmania, Launceston, 7248, Australia*
[c] *Department of Mechanical Engineering, School of Technology, GSFC University, Vadodara, Gujarat, India*

ARTICLE INFO

Method name:
Many-objective meta-heuristic methods

Keywords:
Structural design
Constraint optimization
Evolutionary methods
Natural frequency
Buckling

ABSTRACT

Many-objective truss structure problems from small to large-scale problems with low to high design variables are investigated in this study. Mass, compliance, first natural frequency, and buckling factor are assigned as objective functions. Since there are limited optimization methods that have been developed for solving many-objective truss optimization issues, it is important to assess modern algorithms performance on these issues to develop more effective techniques in the future. Therefore, this study contributes by investigating the comparative performance of eighteen well-established algorithms, in various dimensions, using four metrics for solving challenging truss problems with many objectives. The statistical analysis is performed based on the objective function best mean and standard deviation outcomes, and Friedman's rank test. MMIPDE is the best algorithm as per the overall comparison, while SHAMODE with whale optimisation approach and SHAMODE are the runners-up.

- A comparative test to measure the efficiency of eighteen state-of-the-practice methods is performed.
- Small to large-scale truss design challenges are proposed for the validation.
- The performance is measured using four metrics and Friedman's rank test.

Specifications table

Subject area:	Computer Science
More specific subject area:	*Engineering optimization*
Name of your method:	*Many-objective meta-heuristic methods*
Name and reference of original method:	*Multi-Objective Passing Vehicle Search algorithm for structure optimization* https://www.sciencedirect.com/science/article/abs/pii/S0957417420311556
Resource availability:	*NA*

* Corresponding author.
E-mail address: p.shyam23@gmail.com (G.G. Tejani).
Social media: (G.G. Tejani)

https://doi.org/10.1016/j.mex.2023.102181
Received 2 November 2022; Accepted 11 April 2023
Available online 18 April 2023

Background

Meta-heuristics (MHs) methods are comprehensive optimizer paradigms or black-box methods that might be used for nearly all optimisation issues. As a result, several MHs have been developed over time and are frequently utilized to solve real-world challenging optimization issues [1]. The rationale for its robust search mechanism is its simple and easy execution, gradient-free characteristics, and the balance between its two search blueprints: local intensification (exploitation) and global diversification (exploration) [2]. They also showed their superior performance while addressing multi-objective optimization problems (MOOPs), since they demonstrated their better potential in finding a Pareto front in a single optimization cycle [3–5].

However, a large-scale design challenge such as truss optimization problems with many design variables may make employing MHs challenging [6,7]. Moreover, the search capacity of MHs deteriorated significantly as the number of objectives increased, thus, this poses challenges diversity, convergence, and computational complexity. A category of MOOPs with four or more objectives is called many-objective optimization problems (MaO-OPs) [8]. These issues can be frequently noticed in real-life engineering and industrial design issues such as indirect irradiated solar receiver modeling and optimization [9], automotive engine calibration problems [10], water distribution systems [11], control system design [12], flow shop scheduling problem [13], truss optimization [14], and land use management problem [15]. It comes as no surprise that managing multiple objectives has been a major focus of research among the academic community in recent times, given the complexity that arises from handling a large number of objectives. Literature shows that while implementation of widely used Pareto-dominance based evolutionary approaches like NSGA-II [16] and SPEA2 [17] to problems with so many objectives may cause significant challenges [18,19]:

1. The problem of becoming non-dominated by virtually all solutions in each population eventually results in severe convergence ability deterioration.
2. Convergence and diversification conflict aggravation due to objective space dimensionality exponential increase.
3. The possibility of least efficient offspring generation in high-dimension objective space due to constraints on population size posed by computational efficiency concerns.
4. Significant rise in computational complexity with Hypervolume (HV)-based performance estimation.
5. Difficulty in solution visualization that might face by a decision-maker (DM).

To alleviate the aforementioned challenges and scalability of optimization techniques to address MaO-OPs typically three avenues were adopted in the literature. First is the method of enhancement of the selection process in the direction of the Pareto front (PF) by modifying Pareto-dominance, allocating various rankings to non-dominated solutions, utilization of various fitness assessment techniques [20–22]. The second avenue is the incorporation of preference mechanism [23,24], and the third one is the reduction of objective space (by decreasing objectives numbers) such as decomposition-based mechanism [25–27]. Several MHs have been established in recent years to answer MaO-OPs, but, they are typically limited to unconstrained benchmarks [28]. Moreover, real-world MaO-OPs are comprised of several design restrictions and conflicting objectives that made them more challenging. Consequently, there is a need to examine the key performance measure (i.e., the balance of diversification and intensification) of MHs algorithms for practical challenging MaO-OPs.

A truss is a structure designed to sustain large loads, prevent deflection, and achieve long spans with minimal weight having applications in bridges, ceilings, industrial buildings, towers, etc. Due to its wide engineering applications, lots of research efforts regarding design optimization (both single-& multi-objectives) of the truss have been reported in the literature over the last two decades. The truss mass, nodal displacement, natural frequency, compliance, and frequency response function are often utilized objectives, whereas size, shape, and topology are design variables that were integrated separately or concurrently. The truss is subjected to a variety of mechanical behaviours when in use, including stress, displacement, buckling, and vibration thus these are typical design constraints accounted for optimization in studies. However, due to the inclusion of these constraints, the optimization problem becomes more implicit, non-linear, and non-convex which is often too complicated to solve. Thus, derivative-free MHs are executed for solving these problems which showed high success rates in finding an optimal solution with easiness and flexibility [29–34].

A typical conventional single-objective truss optimization issue has the goal to minimize mass while accounting for numerous design constraints for the truss's safety needs under various loading circumstances. However, the optimal solutions reported were found to lie on constrained edges (i.e. at the threshold of safety and failure) and thus erratic. To resolve such issues multi-objective (MO) design approaches were adopted by including a structure reliability indicator as another objective with mass [35]. MOOPs are frequently investigated in literature as they more or less mimic the real-world environment. Contrary to a single objective they pose heaps of optimal solutions often called a Pareto set, based on which DM makes its choice. As stated before, MH shows its competency while solving these MOOPs and is thus significantly investigated for truss optimization problems. A few notable examples are Heat Transfer Search (HTS) [6,7,36], Genetic Algorithm [37,38], Passing Vehicle Search (PVS) [3], Immune Algorithm [39], HTS-PVS [4], Adaptive Symbiotic Organisms Search [40], Plasma Generation Optimizer [41], Chaotic meta-heuristic algorithm [42], Nature inspired optimization tools for optimization [43] and Modified Differential Evolution (DE) [44].

The real-world truss design problems pose many load cases that result in many reliabilities objectives inclusion such as structural compliance, natural frequencies, and buckling factor. This rise in the number of objectives eventually leads the truss design problems towards MaO-OPs. With several competing goals, the complexity of the design grows rapidly in size, making the truss optimization problem quickly intractable and challenging to solve. Despite such significant engineering and industrial design issue, MaO-OPs of truss structure is lacking in the literature. Pholdee *et al.* [14] first performed a baseline investigation for many-objective truss optimization. However, apart from that, very limited further investigation has been made so far [45,46]. Recently a considerable

number of novel MHs have been developed however their efficacy and utility for many-objective truss optimization have yet to be examined.

The current study has therefore examined a performance comparison of recently proposed many-objective MHs for MaO-OPs of the truss structure. Concurrently, for static and dynamic applications, an examination of the size optimization of the truss was performed. The design problem poses four objective functions viz. mass, compliance, first natural frequency, and compression-buckling ratio subjected to numerous design constraints. Eighteen distinguished MHs viz. MOALO [47], MODA [48], MOGOA [49], MOGWO [50], MOMVO [51], MOWCA [52], MSSA [53], SHAMODE [54], SHAMODE-WO [54], NSGA-II [16], RPBILDE [55], DEMO [56], MOEA/D [57], UPS-EMOA [58], NSGA-III [28], RVEA [23], MnKnEA [22], and MMIPDE [35] are evaluated . Eight widely used planar and spatial truss benchmark structures are examined based on four performance measures.

This study contributes as follows:

- A real-world many objective structures design optimization model is proposed and investigated having four conflicting objectives subjected to several design constraints.
- An extensive performance study of eighteen popular MHs with complicated eight planar and spatial trusses with diverse properties is conducted.
- Four performance metrics and the convergence history of all algorithms are examined for all algorithms.
- A popular Friedman's rank test is performed to get a statistical measure of the eighteen distinguish algorithms.

Method details

To solve MaO-OPs regarding the truss, eighteen MHs are employed. These optimization methodologies are stated to be well-established, with some being regarded as the finest optimisers for solving constrained many-objective test problems. All evaluatedMHs and their basic approach are explained as follows:

MO ant lion optimiser (MOALO) [47]

Inspired by MOPSO, MOALO incorporates a leader selection and archive maintenance mechanism. A repository of PFs is maintained here, where a roulette wheel method is employed to choose a non-dominated solution (NDS) from the archive. Convergence is derived from basic ALO that mimics the antlion's hunting behaviour and their interaction with their prey (ants). Niching technique is utilized for solution distribution assessment in the archive. Like MOPSO, the leaders (antlions) opted to have the least populated territory. The most populous solutions are eliminated when the archive is full to make room for new solutions.

MO dragonfly algorithm (MODA) [48]

A MO variation of swarm intelligence-based DA is known as MODA. During the optimization process, an archive is provided for storing and retrieving the best approximate NDS. Here the positions are updated similarly to DA while the source of food is selected from the repository. The convergence and coverage behaviour of MODA is inspired by MOPSO. Segments of search space are created to locate the solutions in the least populated regions whereas leader selection is done as per the mechanism of a roulette wheel.

MO grasshopper optimisation algorithm (MOGOA) [49]

Inspired by GOA's efficient peculiar adaptive method that creates a harmony between exploration and exploitation, MOGOA was developed. The natural swarming behaviour of grasshoppers is mathematically modelled for MOOPs. To convert the basic GOA into a MO version an archive and target selection methodology is incorporated similar to MOPSO in MOGOA that helps in finding PFs.

MO grey wolf optimiser (MOGWO) [50].

MOGWO mimics the grey wolf hunting approach and their social hierarchy. Analogous to MOPSO, two components i.e. archive and leader selection mechanism is adopted for a transition of basic GWO into a MO version. To store and maintain the NDS external archive is used whereas to improve the repository results a grid mechanism is integrated with basic GWO. Here leader selection methodology is implemented (based on 3 best results viz. α, β, and δ) to upgrade and replace PFs.

MO multiverse optimisation (MOMVO) [51]

It is inspired by the physics hypotheses postulating the possibility of multiple universes and simulating their interaction. Equivalent to MOPSO and PAES, a roulette wheel-based leader selection method is incorporated to update and select the NDS, and an archive is utilized to keep these solutions. Here white, black, and wormholes are taken as references for other solutions position updates.

MO water cycle algorithm (MOWCA) [52]

MOWCA is founded on the premise of the natural water cycle phenomenon and replicates the passage of streams and rivers toward the sea. A crowding distance method is employed here to select the best solution that includes rivers and seas. Furthermore, to construct PFs, NDS are preserved in the archive.

MO Salp swarm algorithm (MSSA) [53]

MSSA imitates a navigating and foraging action of salps in the sea by forming a salp chain. The front salp of the chain is the leader which guides the remaining slaps (followers) towards the food source. Identical to MOPSO, MSSA stores the best NDS in an archive (repository) obtained during optimization. The leader is selected through the ranking process and employment of roulette wheel methodology based on which the position of other salps is modified.

Success history-based adaptive MO DE (SHAMODE) [54]

SHAMODE is the MO method of the SHADE algorithm that employs the self-adaptive technique for controlling parameter tuning of DE. Based on the success history memory new controlling parameter values is adapted that improve search efficiency. It starts with population initialization and the formation of an external archive. Both are updated iteratively as per DE operators and new NDS are stored in the repository. The search ends after reaching the termination criteria and the most updated solutions obtained are set equal to the approximate PFs.

Success history-based adaptive MO DE with whale optimisation (SHAMODE-WO) [54]

To enhance SHAMODE search diversity, the spiral motion operator of the Whale Optimization Algorithm is combined with the binomial crossover of DE. Here the mutation vector is get updated to a new mutation vector according to the spiral movement technique before the implementation of a crossover step.

NSGA-II [16]

NSGA-II is an upgradation of NSGA and perhaps the most widely acknowledges MOEA. To upgrade the NSGA convergence property, here an Elitism mechanism is incorporated. Identical to GA, this method creates offspring sets from the parent with crossover and mutation operators. The solution updating procedure is repeated until the stop condition is met. The search efficiency is enhanced by using NDS and crowding distance mechanism.

Hybridisation of real-code population-based incremental learning and DE (RPBILDE) [55]

RPBILDE is a hybrid MO evolutionary algorithm that was generated by integrating the DE operator into the basic approach of RPBIL. The population is generated based on a probability matrix initially which is then hybridized with existing NDS. Here both the probability matrix and NDS keep on updating unit termination condition is not reached.

DE for MO optimisation (DEMO) [56]

DEMO is a MO variant of DE that merges the benefits of DE with Pareto-based ranking and crowd distance sorting methods. Alike NSGA-II, DEMO assumes the elitism approach. The key dissimilarity is that it uses DE based mutation and crossover, rather than genetic algorithm procedures..

MO evolutionary algorithm based on decomposition (MOEA/D) [57]

MOEA/D is another famous MOEA that uses the basic scalarization technique. Here the MOOPs are explicitly decomposed into scalar subproblems that are optimized simultaneously by using neighbour scalar aggregation function information. Moreover, like other population-based MH methodologies, it uses a NDS method to obtain PFs. Iterative updating of solutions ends after reaching the termination criteria.

Unrestricted population size evolutionary MO optimisation algorithm (UPS-EMOA) [58]

As the name suggested UPS-EMOA allowed a peculiar greater size of PF against the widely used solution filtering approach of MHs to maintain constant archive size. The notion here is to enhance the solution diversity by increasing the number of solutions. For creating offspring, the DE operator is used while solutions are stored in a repository that allowed storage of solutions according to computer capacity.

Reference-point-based many-objective evolutionary algorithm (NSGA-III) [28]

To make NSGA-II compatible with MaO-OPs, an improved version called NSGA-III is developed. A predefined reference point set that serves as a reference allocation for the final output is used in NSGA-III for diversity maintenance. In solution selection, the NSGA-III uses the least perpendicular distances to these reference locations as a criterion. In another word, it highlights non-dominated population members who are close to reference points.

Reference vector guided evolutionary algorithm for MaO-OPs (RVEA) [59]

RVEA employs the elitism technique for population generation and selection, much like NSGA-II. Conventional crossover and mutation procedure of GA is applied to create the offspring population. To achieve a balance between convergence and diversity, the angle penalized distance scalarization technique, like MOEA/D, is employed here. Moreover, these reference vectors distribution is dynamically adjusted based on adaptive and regeneration techniques. Here the predefined reference vectors set can be uniformly generated or user preference specified.

Knee point driven evolutionary algorithm for MaO-Ops (MnKnEA) [60]

MnKnEA uses knee point as a additional guideline for selecting next-generation parents apart from the non-dominance selection procedure. In absence of user-specific presences, knee points which is the PFs subset are naturally preferred for selection in every population. This is the rough illustration of preference mechanism bias towards larger HV that eventually helps in setting the convergence and diversity of the search. Knee points are identified based on an adaptive strategy here.

MO meta-heuristic with iterative parameter distribution estimation (MMIPDE) [61]

MMIPDE is a dominance-based MO MHs that has a self-adaptive mechanism achieved through distribution evaluation. A modified DE reproduction technique is used while the controlling parameters are estimated based on a population-based incremental learning approach. The algorithm starts with the initialization of a probability matrix and initial Pareto archive. Based on a NDS scheme, high- and low-level archives update iteratively. The algorithm stops when termination criteria is reached.

The aforementioned algorithms MATLAB codes are primarily given by their developers; however, some are developed by the authors of this study. To have a fair comparison between all evaluated optimization techniques, authors employed analogous hardware and computer language.

Problem statement

A mathematical programming problem of truss structure can be stated as follows.

$$Find,\ X = \{A_1,\ A_2, .., A_m\} \tag{1}$$

To minimize the mass of truss, minimize compliance, maximize first natural frequency, and minimize maximum buckling factor:

$$F_1(X) = mass = \sum_{i=1}^{m} A_i \rho\ L_i \tag{2}$$

$$F_2(X) = compliance = \delta^T * F \tag{3}$$

$$F_3(X) = inverse\ of\ first\ natural\ frequency = 1/f_1 \tag{4}$$

$$F_4(X) = maximum\ buckling\ factor = \max\left(\frac{\left|\sigma_j^{comp}\right|}{\sigma_j^{cr}}\right), \tag{5}$$

Subject to:
Behavior constraints:

$$g_1(X) : Stress\ constraints,\ \frac{\max\left(\left|\sigma_j\right|\right) - \sigma_{allowable}}{\sigma_{allowable}} \le 0 \tag{6}$$

$$g_2(X) : Euler\ buckling\ constraints,\ \max\left(\frac{\left|\sigma_j^{comp}\right| - \sigma_j^{cr}}{\sigma_j^{cr}}\right) \le 0,\ where\ \sigma_j^{cr} = \frac{kA_jE}{L_j^2} \tag{7}$$

Side constraints:

$$Cross - sectional\ area\ constraints,\ A_i^{min} \le A_i \le A_i^{max} \tag{8}$$

where,

A_i *is a cross-section of i-th element*
A_i^{min} *is a minimum value of A*
A_i^{max} *is a maximum value of A*
ρ *is a density of truss material*
L_i *is a length of i-th truss member*
δ *is a displacement vector from finite element analysis*
F *is a load vector from finite element analysis*
f_1 *is the first natural frequency*
σ_i^{comp} *is compressive stress of i-th truss member*
σ_i^{cr} *is critical compressive stress of i-th truss member*
i *is an index of a compressive truss member*
m *is number of compressive truss members*
j *is an index of a degrees of freedom*
n *is number of degrees of freedom*
k *is Euler buckling coefficient which is set to 3.96*
σ_i^{cr} *is allowable buckling stress of i-th compressive member*
E *is the modulus of elasticity*
A_i *is the cross-section area of i-th compressive member.*
L_i *is the length of the i-th compressive member*

Elemental cross-sections are assumed to be countable variables as beam regular sections which ensure the practicability of the structure. The ground structure of the 10–, 25–, 37–, 60–, 72–, 120–, 200–, and 942–bar trusses are presented in Figs. 1–4. Certain elements of the evaluated trusses are grouped as per the structural symmetricity. Therefore, the numbers of design variables of the 10– bar truss, 25– bar truss, 37– bar truss, 60– bar truss, 72– bar truss, 120– bar truss, 200– bar truss, and 942–bar truss are taken into 10 groups, 8 groups, 15 groups, 25 groups, 16 groups, 7 groups, 29 groups, and 59 groups respectively. It is assumed that the properties and permittable limits of all trusses are the same. Mass Density, elastic modulus, and permittable stress are assumed as 7850 kg/m^3, 200 GPa, and 400 MPa respectively. The design considerations such as design variables, material density, Young's modulus, constraints, and loading conditions are shown in Table 1.

Table 1
Design considerations of the truss problems.

	The 10-bar truss	The 25-bar truss	The 37-bar truss	The 60-bar truss	The 72-bar truss	The 120-bar truss	The 200-bar truss	The 942-bar truss
Design variables	$A_{i,} i = 1, 2, \dots, 10$	$A_{i,} i = 1, 2, \dots, 8$	$A_{i,} i = 1, 2, \dots, 15$	$A_{i,} i = 1, 2, \dots, 25$	$A_{i,} i = 1, 2, \dots, 16$	$A_{i,} i = 1, 2, \dots, 7$	$A_{i,} i = 1, 2, \dots, 29$	$A_{i,} i = 1, 2, \dots, 59$
Stress Constraints	σ^{max} = 400 MPa	σ^{max} = 400 MPa	σ^{max} = 400 MPa	σ^{max} = 400 MPa	σ^{max} = 400 MPa	σ^{max} = 400 MPa	σ^{max} = 400 MPa	σ^{max} = 400 MPa
Density	ρ = 7850 kg/m^3	ρ = 7850 kg/m^3	ρ = 7850 kg/m^3	ρ = 7850 kg/m^3	ρ = 7850 kg/m^3	ρ = 7850 kg/m^3	ρ = 7850 kg/m^3	ρ = 7850 kg/m^3
Young's modulus	E = 200 GPA	E = 200 GPA	E = 200 GPA	E = 200 GPA	E = 200 GPA	E = 200 GPA	E = 200 GPA	E = 200 GPA
Size variables	$A_{i,} \in S$, $i = 1, 2, \dots, 10$ S =[1, 1.5, 2, …,21] *1e-3 m^2	$A_{i,} \in S$, $i = 1, 2, \dots, 8$ S =[1, 1.5, 2, …,21] *1e-3 m^2	$A_{i,} \in S$, $i = 1, 2, \dots, 8$ S =[1, 1.5, 2, …,21] *1e-3 m^2	$A_{i,} \in S$, $i = 1, 2, \dots, 8$ S =[1, 1.5, 2, …,21] *1e-3 m^2	$A_{i,} \in S$, $i = 1, 2, \dots, 8$ S =[1, 1.5, 2, …,21] *1e-3 m^2	$A_{i,} \in S$, $i = 1, 2, \dots, 8$ S =[1, 1.5, 2, …,21] *1e-3 m^2	$A_{i,} \in S$, $i = 1, 2, \dots, 8$ S =[1, 1.5, 2, …,21] *1e-3 m^2	$A_{i,} \in S$, $i = 1, 2, \dots, 59$ S =[1, 1.5, 2, …,21] *1e-1 m^2
Loading conditions	$P_{y2} = P_{y4} =$ −1000 KN	$P_{x1} = 100\ KN$, $P_{y1} = P_{z1} = P_{y2} = P_{z2} = -1000\ KN$, $P_{x3} = 50\ KN$, $P_{x6} =$ 60 KN	$P_{y2}, P_{y3}, P_{y4}, \dots, P_{y10} = -100\ KN$	Case 1: $P_{x1} = -1000\ KN$, $P_{x7} = 900\ KN$ Case 2: $P_{x15} = P_{x18} = -800\ KN$, $P_{y15} = P_{y18} = 300\ KN$ Case 3: $P_{x22} = -2000\ KN$ and $P_{y22} = 1000\ KN$	Case 1: $F_{17x} = F_{17y} =$ 2000 KN, $F_{17z} =$ − 2000 KN Case 2: $F_{17z} = F_{18z} = F_{19z} = F_{20z} =$ −2000 KN	$P_{z28}, P_{z29}, P_{z30}, \dots, P_{z36} = -500\ KN$, $P_{z37}, P_{z38}, P_{z39}, \dots, P_{z48} = -1500\ KN$, $P_{z49} = -3000\ KN$	$P_{x1}, P_{x6}, P_{x15}, P_{x20}, P_{x29}, P_{x34}, P_{x43}, P_{x48}, P_{x57}, P_{x71} = 10\ KN$ $P_{y1}, P_{y2}, \dots, P_{y6}, P_{y8}, P_{y10}, P_{y12}, P_{y14}, P_{y15}, \dots, P_{y20}$ $P_{y22}, P_{y24}, P_{y26}, P_{y28}, P_{y29}, \dots, P_{y34}, P_{y36}, P_{y40}, P_{y36}, P_{y38}, P_{y40}, P_{y42}, P_{y43}, \dots, P_{y48}$ $P_{y50}, P_{y52}, P_{y54}, P_{y56}, P_{y57}, \dots, P_{y62}, P_{y64}, P_{y66}, P_{y68}, P_{y70}, P_{y71}, \dots, P_{y75}, = -100\ KN$	At each node: vertical loading: Section 1; P_z = −6 KN Section 2; P_z = −12 KN Section 3; P_z = −18 KN Lateral loading: Right-hand side; P_x = 3 KN Left-hand side; P_x = 2 KN Lateral Loading: P_y = 2 KN

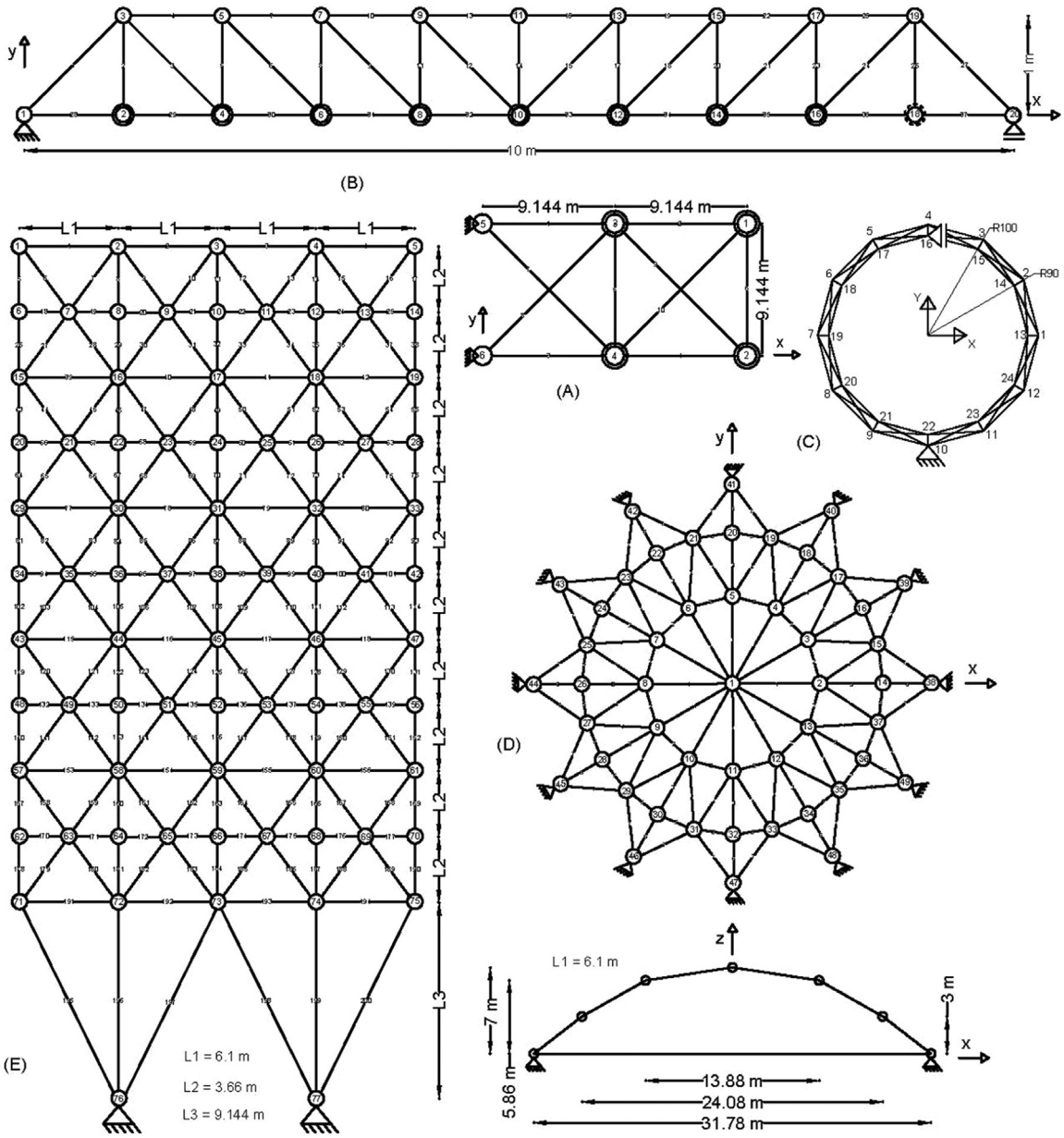

Fig. 1. Trusses: (A) 10-bar truss, (B) 37-bar truss, (C) 60-bar truss, (D) 120-bar truss, and (E) 200-bar truss.

The HV, Generational Distance (GD), Inverted GD (IGD), and Spacing-to-Extent (STE) are taken as performance metrics to measure the comparative performance. HV calculates the spread and advancement of a PF. GD and IGD calculate distances between an obtained PF and a reference front while STE measures the ratio of spacing to extent of a front. Here, the reference front of each problem is NDS gathered from the results of all optimizations run.

The HV indicator is the volume in hyper-space between the reference point and PF. The reference point is the extremum point gathered from the union of all obtained solutions. HV can be calculated with Eq. (9).

$$HV = \cup_{i=1}^{|NP|} V_i \tag{9}$$

where, V_i is the volume between *i-th* NDS and the reference. The higher HV indicates better spread and/or advancement of PF.

The *GD* and *IGD* are performance indicators examined and stated in Eq. (10) and Eq. (11):

$$GD = \frac{\sqrt{\sum_{i=1}^{|NP|} ED_i{}^2}}{|NP|} \tag{10}$$

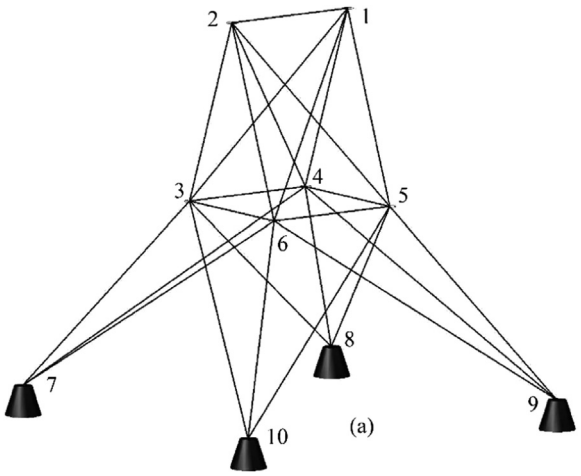

Fig. 2. The 25-bar 3D truss.

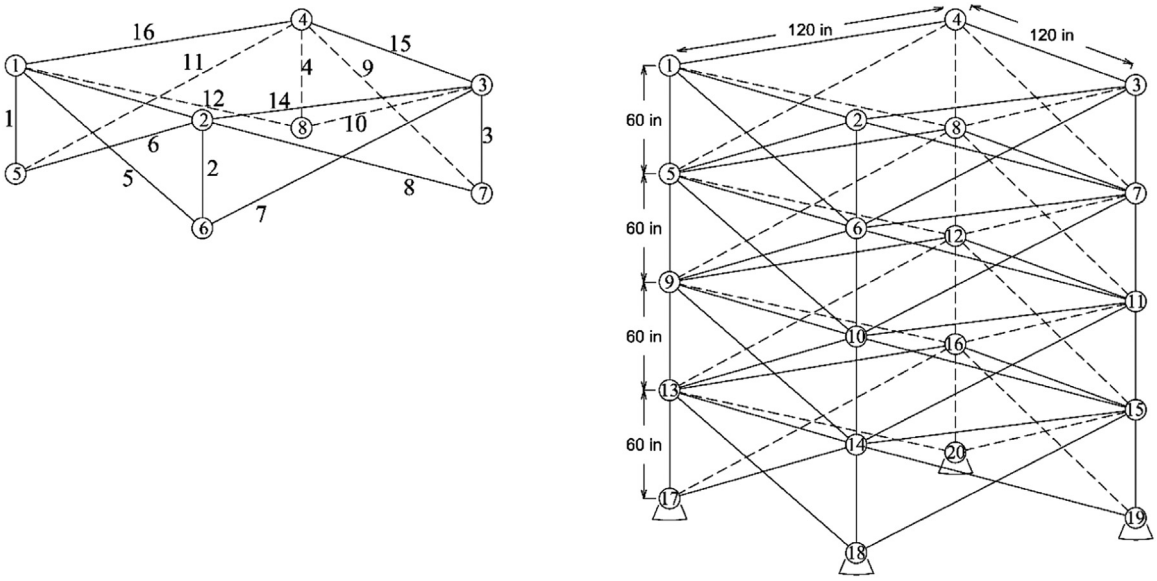

Fig. 3. The 72-bar 3D truss.

$$IGD = \frac{\sqrt{\sum_{i=1}^{|NP'|} {ED'}_i^2}}{|NP|} \tag{11}$$

where $|NP|$ and $|NP'|$ indicates the obtained PF and the reference PF count respectively. ED_i is the Euclidian distance measured between the i^{th} solution in obtained PF and the nearest solution in true PF while ${ED'}_i$ is the Euclidian distance measured between the i^{th} solution of true PF and the closest solution from obtained PF. Both GD and IGD indicate distance from the obtained front and the reference front, but in different manner. The Pareto with lower GD and IGD is closer to the reference front.

The Front Spacing-to-Extent is the ratio between spacing to extent which calculated with Eq. (12).

$$\text{Front Spacing} - \text{to} - \text{Extent (FSTE)} = \text{Spacing/Extent} = \frac{\frac{1}{|NP|-1}\sum_{i=1}^{|NP|}\left(d_i - \bar{d}\right)^2}{\sum_{j=1}^{M}\left|f_j^{max} - f_j^{min}\right|} \tag{12}$$

Where, d_i is Euclidian distance of *i-th* objective function vector from obtained Pareto to its closest adjacent, $\bar{d}$ is mean value of d_i, f_j^{max} is the highest value, and f_j^{min} is the lowest value. The lower spacing values indicates superior PF while the higher values of extent represent better extension. By combining both metrics, the FSTE metric can indicate quality of a PF in both spacing and extension aspect.

Here, four metrics are tested to measure performance of algorithms in different aspect. Lower values of *GD, IGD*, and *FSTE* represent better PF while the *HV* with higher values is better.

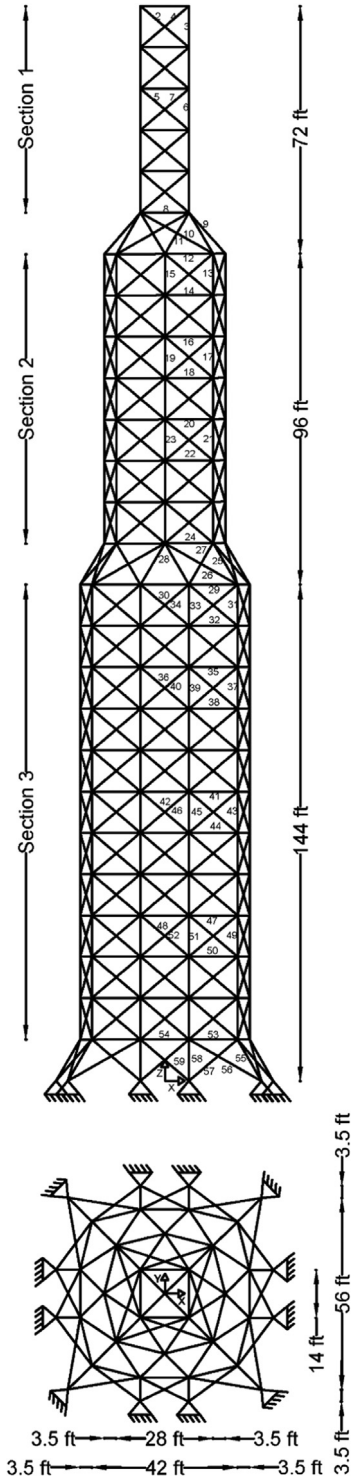

Fig. 4. The 942-bar tower truss.

Table 2
Mean hypervolume obtained from the eighteen algorithms (the bold indicates the best solution).

Mean HV	10-bar	25-bar	37-bar	60-bar	72-bar	120-bar	200-bar	942-bar
MOALO	1.1569E+09	5.5507E+08	2.0671E+08	3.7422E+08	1.8157E+09	4.4132E+10	5.0260E+09	1.7696E+14
MODA	1.1866E+09	7.7936E+08	2.2954E+08	5.4899E+08	2.5538E+09	6.3648E+10	5.9429E+09	1.6556E+14
MOGOA	1.4709E+09	6.3441E+08	2.1170E+08	5.3963E+08	2.4820E+09	5.8884E+10	6.1080E+09	1.9051E+14
MOGWO	1.1697E+09	4.7264E+08	1.5390E+08	5.3081E+08	2.3276E+09	4.1554E+10	1.0438E+10	3.3152E+14
MOMVO	2.6981E+09	1.2515E+09	3.5168E+08	1.1022E+09	5.1416E+09	7.1977E+10	1.4825E+10	4.5000E+14
MOWCA	1.5012E+09	6.2957E+08	2.3379E+08	7.2933E+08	3.2077E+09	7.9572E+10	8.6812E+09	2.3225E+14
MSSA	1.2643E+09	5.0571E+08	1.8632E+08	6.0835E+08	2.6408E+09	4.5320E+10	6.6409E+09	1.8404E+14
SHAMODE	7.3578E+09	2.8587E+09	8.4253E+08	2.4381E+09	9.5994E+09	2.8284E+11	2.1764E+10	5.0047E+14
SHAMODE-WO	6.7284E+09	2.7440E+09	8.0726E+08	2.4371E+09	1.1161E+10	2.8106E+11	2.6122E+10	**8.9145E+14**
NSGA-II	2.2553E+09	1.1044E+09	3.6532E+08	9.7769E+08	2.7930E+09	9.5935E+10	9.7116E+09	2.1618E+14
RPBILDE	5.4344E+09	2.4479E+09	7.4257E+08	2.3228E+09	9.9342E+09	2.5049E+11	2.4631E+10	5.8492E+14
DEMO	2.2955E+09	9.3215E+08	4.1299E+08	7.3093E+08	3.0482E+09	8.2183E+10	1.0483E+10	3.3517E+14
MOEA/D	1.1513E+09	6.3847E+08	1.9737E+08	6.2943E+08	2.5673E+09	4.0995E+10	1.2761E+10	2.2980E+14
UPSEMOA	2.4626E+09	8.4241E+08	4.9260E+08	1.0965E+09	3.1990E+09	1.0267E+11	1.0434E+10	3.6855E+14
NSGA-III	1.8658E+09	8.5182E+08	2.3078E+08	8.0817E+08	4.0170E+09	1.2652E+11	1.1527E+10	3.2636E+14
RVEA	1.0710E+09	4.3762E+08	1.6977E+08	2.4430E+08	1.5193E+09	5.9003E+10	3.9219E+09	1.1875E+14
MnKnEA	1.0046E+09	6.0190E+08	3.9344E+08	1.0889E+09	2.2821E+09	2.5969E+11	6.6643E+09	1.9059E+14
MMIPDE	**8.5526E+09**	**3.5510E+09**	**9.4471E+08**	**3.3886E+09**	**1.4015E+10**	**3.4300E+11**	**2.6236E+10**	3.0391E+14

Table 3
Standard deviation of hypervolume obtained from the eighteen algorithms (the bold indicates the best solution).

STD of HV	10-bar	25-bar	37-bar	60-bar	72-bar	120-bar	200-bar	942-bar
MOALO	2.7776E+08	1.7736E+08	4.7655E+07	**3.2834E+07**	5.7410E+08	1.2012E+10	6.7629E+08	**6.4719E+09**
MODA	3.0421E+08	2.4157E+08	5.4874E+07	8.9850E+07	8.1571E+08	1.1323E+10	9.2086E+08	7.9380E+09
MOGOA	4.8583E+08	1.5476E+08	5.6265E+07	9.1157E+07	5.3977E+08	1.8179E+10	9.8976E+08	1.2394E+10
MOGWO	1.1574E+08	**7.1626E+07**	2.9801E+07	6.0604E+07	5.4675E+08	**6.1858E+09**	1.7915E+09	2.3127E+10
MOMVO	9.8099E+08	5.2932E+08	9.8997E+07	3.1918E+08	2.3930E+09	3.1222E+10	5.3996E+09	3.4144E+10
MOWCA	6.7942E+08	2.6378E+08	6.5811E+07	1.6829E+08	8.7991E+08	2.8921E+10	2.0343E+09	1.3677E+10
MSSA	2.6518E+08	9.4505E+07	4.7568E+07	1.0582E+08	8.0461E+08	1.8820E+10	1.4321E+09	7.8607E+09
SHAMODE	1.0628E+09	2.6342E+08	8.5638E+07	3.5414E+08	1.8934E+09	2.9074E+10	3.2369E+09	2.1001E+10
SHAMODE-WO	1.0564E+09	2.9142E+08	8.4359E+07	3.8500E+08	1.8922E+09	2.9803E+10	3.9778E+09	4.7654E+10
NSGA-II	6.1738E+08	3.4470E+08	8.4958E+07	2.7085E+08	8.7264E+08	3.1762E+10	1.9589E+09	6.6350E+09
RPBILDE	1.2225E+09	3.6316E+08	1.0673E+08	3.0667E+08	1.6112E+09	3.0704E+10	5.7064E+09	4.6584E+10
DEMO	8.4052E+08	2.6188E+08	8.7071E+07	1.3386E+08	6.2494E+08	1.9987E+10	3.5405E+09	2.8079E+10
MOEA/D	2.3375E+08	1.2787E+08	2.9406E+07	1.2376E+08	3.7858E+08	7.6319E+09	4.8808E+09	3.9894E+10
UPSEMOA	7.5497E+08	2.0112E+08	1.0943E+08	2.0055E+08	8.3086E+08	2.4422E+10	1.5545E+09	1.8042E+10
NSGA-III	4.6099E+08	2.2121E+08	6.3869E+07	1.9971E+08	8.4320E+08	3.6780E+10	1.5693E+09	1.8928E+10
RVEA	1.7100E+08	1.1545E+08	**1.9469E+07**	1.4350E+08	**2.2020E+08**	1.3112E+10	7.7930E+08	8.2212E+09
MnKnEA	**9.1670E+07**	2.5969E+08	5.9871E+07	1.4728E+08	4.1002E+08	3.0380E+10	**5.7240E+08**	7.5733E+09
MMIPDE	1.8228E+09	3.1080E+08	8.0064E+07	4.4363E+08	1.9393E+09	3.1064E+10	4.7640E+09	8.1560E+10

Method validation

The eighteen considered algorithms are tested with 30 separate runs of each of the algorithms. All the considered trusses are investigated by assuming a population size of 100 and with the termination criteria being a maximum of 10000 function evaluations. The algorithms used in this study are gathered from two sources i.e. the best-known algorithms and newly published MO meta-heuristics. Eight well-known truss optimisation problems with four objectives and two constraints are used to test the considered algorithms. The HV, GD, IGD, and STE performance indicators are used to test the performance. Also, Friedman's rank test is carried out to support the four performance indicators. Most of the optimization algorithms were downloaded from their authors, thus, the default parameters settings by those researchers are used. Nevertheless, there are five algorithms NSGA-II, RPBILDE, DEMO, MOEA/D, and UPSEMOA that were coded by the authors where their parameter settings can be found in [55]. The traditional exterior penalty function method is used to manage the design constraints with the exception of SHAMODE, SHAMODE-WO, NSGA-II, RPBILDE, DEMO, MOEA/D, UPSEMOA, and MMIPDE where the constraint handling approach in [59] is embedded to their codes.

The solutions obtained mean values of HV, GD, IGD, and STE are presented in Tables 2, 5, 8, and 11 whereas the standard deviation (STD) values of HV, GD, IGD, and STE are presented in Tables 3, 6, 9, and 12. Friedman's rank test is used to rank the algorithms as a statistical review and solutions are presented in Tables 4, 7, 10, and 13 respectively. The bold indicates the best solution obtained for each of the problems. As stated previously, a higher value of HV discloses the better solutions while a lower value of GD, IGD, and STE indicated better solutions.

Table 2 presents the mean HV obtained from the eighteen algorithms. It is noticed from the table that MMIPDE obtains the best solutions in 10–bar, 25–bar, 37–bar, 60–bar, 72–bar, 120–bar, and 200–bar trusses while SHAMODE-WO obtains the best solution for the remaining 942–bar truss. Table 3 presents STD of HV obtained from the eighteen algorithms. It is noticed from the table that MOALO obtains the best solutions in 60–bar and 942–bar trusses, MOGWO obtains the best solutions in 25–bar and 120–bar trusses,

Table 4
Friedman's rank of hypervolume obtained from the eighteen algorithms (the bold indicates the best solution).

Friedman's rank of HV	10-bar	25-bar	37-bar	60-bar	72-bar	120-bar	200-bar	942-bar	Overall Friedman's value	Overall Friedman rank
MOALO	13.37	13.50	13.07	16.73	15.03	15.40	15.00	16.80	118.90	17
MODA	13.27	9.73	12.13	13.43	11.23	11.53	13.90	14.33	99.57	12
MOGOA	11.00	11.70	12.90	13.90	11.50	13.07	13.33	12.43	99.83	14
MOGWO	13.03	14.87	16.00	13.87	12.30	15.80	8.17	5.77	99.80	13
MOMVO	6.63	6.83	8.20	6.80	6.10	11.30	5.77	4.77	56.40	5
MOWCA	11.57	12.23	11.90	10.37	8.70	10.27	9.97	10.43	85.43	9
MSSA	12.37	14.33	14.00	12.27	10.93	14.73	12.60	13.70	104.93	16
SHAMODE	2.20	2.53	2.47	2.90	3.30	2.60	3.57	5.77	25.33	4
SHAMODE-WO	2.57	2.97	2.83	2.80	2.47	2.80	**2.27**	2.60	21.30	2
NSGA-II	7.43	6.83	7.47	7.63	10.60	8.53	8.90	10.97	68.37	8
RPBILDE	3.57	3.50	3.33	3.13	3.07	3.63	2.73	**1.63**	24.60	3
DEMO	7.50	7.83	6.77	9.93	9.17	9.37	8.40	8.53	67.50	7
MOEA/D	13.23	11.53	13.27	11.90	11.33	15.63	6.93	7.70	91.53	10
UPSEMOA	6.83	8.73	5.93	6.20	8.40	7.90	8.00	6.83	58.83	6
NSGA-III	11.10	11.33	14.17	13.23	11.87	8.13	15.00	13.23	98.07	11
RVEA	16.33	16.47	17.37	17.93	17.57	14.23	17.30	16.20	133.40	18
MnKnEA	17.30	15.03	7.80	6.80	16.17	4.97	16.90	16.17	101.13	15
MMIPDE	**1.70**	**1.03**	**1.40**	**1.17**	**1.27**	**1.10**	**2.27**	3.13	**13.07**	**1**

Table 5
Mean generational distance obtained from the eighteen algorithms (the bold indicates the best solution).

Mean GD	10-bar	25-bar	37-bar	60-bar	72-bar	120-bar	200-bar	942-bar
MOALO	1.4400E+02	8.0219E+01	6.0633E+01	5.9679E+01	1.4198E+02	8.8421E+02	3.6227E+02	9.2777E+02
MODA	1.2786E+02	7.9614E+01	4.6949E+01	6.9243E+01	1.2590E+02	8.2391E+02	3.9014E+02	9.7983E+02
MOGOA	1.3638E+02	8.5465E+01	5.7853E+01	7.5871E+01	1.6532E+02	8.2986E+02	4.2587E+02	1.1377E+03
MOGWO	7.8490E+01	5.0609E+01	**2.2361E+01**	8.4865E+01	8.9190E+01	9.7335E+02	**1.5506E+02**	**7.8809E+02**
MOMVO	8.0339E+01	6.4083E+01	2.9056E+01	6.4133E+01	1.1175E+02	8.3179E+02	3.4293E+02	1.1577E+03
MOWCA	6.5551E+01	6.4413E+01	3.0453E+01	6.6093E+01	1.1512E+02	7.8794E+02	1.9422E+02	8.6543E+02
MSSA	8.9910E+01	7.5377E+01	4.0285E+01	6.4154E+01	1.1811E+02	9.2289E+02	4.0087E+02	9.9194E+02
SHAMODE	8.5749E+01	7.1267E+01	3.6508E+01	6.3965E+01	1.1620E+02	8.4463E+02	1.8271E+02	8.1739E+02
SHAMODE-WO	8.3903E+01	6.8807E+01	3.4880E+01	6.4544E+01	1.2009E+02	8.4567E+02	1.8668E+02	8.1245E+02
NSGA-II	7.0296E+01	5.9627E+01	3.0007E+01	5.5841E+01	8.8083E+01	6.2773E+02	1.9081E+02	8.4026E+02
RPBILDE	8.7698E+01	6.9407E+01	3.9547E+01	6.7725E+01	1.3556E+02	8.6943E+02	2.3914E+02	9.3975E+02
DEMO	7.2100E+01	5.6032E+01	3.9204E+01	**4.6456E+01**	9.0219E+01	6.0782E+02	1.9200E+02	8.2837E+02
MOEA/D	**5.0307E+01**	**4.1783E+01**	2.6925E+01	5.4659E+01	1.8021E+02	**6.0247E+02**	1.7901E+02	1.3133E+03
UPSEMOA	6.2836E+01	4.7715E+01	3.4324E+01	5.2313E+01	**7.9259E+01**	6.2898E+02	1.8472E+02	8.3904E+02
NSGA-III	1.3991E+02	8.4541E+01	5.0309E+01	1.2507E+02	1.6937E+02	9.5622E+02	1.4212E+03	1.9621E+03
RVEA	4.1085E+02	2.1526E+02	1.1290E+02	2.6667E+09	5.3381E+02	1.8489E+03	2.5943E+03	4.2704E+03
MnKnEA	2.0684E+02	1.8488E+02	3.2826E+01	7.2832E+01	2.3489E+02	9.7050E+02	1.2857E+03	2.1579E+03
MMIPDE	9.8400E+01	8.0461E+01	4.5589E+01	6.6108E+01	1.3980E+02	9.2824E+02	2.4243E+02	7.9695E+02

RVEA obtains the best solutions in 37–bar and 72–bar trusses, MnKnEA obtains the best solutions in 10–bar and 72–bar trusses. It is also observed that there is no significant difference in STD when compared with MMIPDE and SHAMODE-WO. Table 4 presents Friedman's rank of HV obtained from the eighteen algorithms. It is noticed from the table that MMIPDE obtains the best solutions in 10–bar, 25–bar, 37–bar, 60–bar, 72–bar, 120–bar, and 200–bar trusses while SHAMODE-WO obtains the best solutions in 942–bar truss. Both MMIPDE and SHAMODE–WO provided the best results in 200–bar truss with equal Friedman's rank. The overall performance of MMIPDE based on HV results is the best among the evaluated MHs and SHAMODE–WO performs second best.

Table 5 presents mean GD obtained from the eighteen algorithms. It is noticed from result table that MOEA/D obtains the best solutions in 10–bar, 25–bar, and 120–bar trusses; MOGWO obtains the best solutions 37–bar, 200–bar, and 942–bar trusses; while DEMO and UPSEMOA obtain the best solutions in 60–bar and 72–bar trusses, respectively. Table 6 presents STD of GD obtained from the eighteen algorithms. It is noticed from the table that MOGWO obtains the best solutions in 10–bar, 25–bar, 37–bar, and 72–bar trusses, while SHAMODE–WO, RPBILDE, SHAMODE, and MMIPDE obtains the best solutions in 60–bar, 120–bar, 200–bar, and 942–bar trusses, respectively. Table 7 presents Friedman's rank of GD obtained from the eighteen algorithms. It is noticed from the table that MOEA/D obtains the best solutions in 10–bar and 25–bar trusses; DEMO obtains the best solutions in 60–bar and 120–bar trusses; MOGWO obtains the best solutions in 37–bar and 200–bar trusses; while UPSEMOA and MMIPDE obtain the best solutions in 72–bar and 942–bar trusses. The overall performance of UPSEMOA based on GD results is the best among the evaluated algorithms whereas NSGA–II performs second best. Also, MMIPDE reported significant performance in solving the large-size trusses.

Tables 8 and Table 9 present mean values and STD of inverted generational distance obtained from the eighteen algorithms. It is noticed from the tables that MMIPDE obtains the best solutions in 25–bar, 37–bar, 60–bar, 72–bar, 120–bar, and 942–bar trusses

Table 6
Standard deviation of generational distance obtained from the eighteen algorithms (the bold indicates the best solution).

STD of GD	10-bar	25-bar	37-bar	60-bar	72-bar	120-bar	200-bar	942-bar
MOALO	3.1462E+01	1.4411E+01	1.8143E+01	7.6371E+00	3.5024E+01	1.5151E+02	8.1195E+01	2.3518E+02
MODA	3.2922E+01	1.1117E+01	1.0868E+01	9.7136E+00	2.2768E+01	1.0351E+02	1.0588E+02	1.4687E+02
MOGOA	2.8911E+01	1.8839E+01	1.3321E+01	1.4537E+01	5.7807E+01	1.4970E+02	1.5103E+02	2.0637E+02
MOGWO	**4.5724E+00**	**2.8489E+00**	**2.2057E+00**	8.4343E+00	**9.6726E+00**	1.0857E+02	1.2536E+01	6.7882E+01
MOMVO	8.2760E+00	1.1582E+01	4.3389E+00	4.9544E+00	1.6882E+01	1.7191E+02	8.2364E+01	1.6173E+02
MOWCA	1.8274E+01	1.6774E+01	3.5943E+00	6.4387E+00	1.2079E+01	1.4603E+02	3.4133E+01	9.0976E+01
MSSA	1.9325E+01	7.3881E+00	6.8544E+00	6.1999E+00	2.8570E+01	1.6739E+02	1.0679E+02	1.1006E+02
SHAMODE	5.0156E+00	4.5669E+00	4.4051E+00	3.9283E+00	1.2086E+01	4.6223E+01	**8.5485E+00**	4.1389E+01
SHAMODE-WO	5.5889E+00	4.1893E+00	4.0149E+00	**2.9352E+00**	1.1004E+01	4.8550E+01	1.1652E+01	4.9961E+01
NSGA-II	7.3481E+00	1.0410E+01	4.1403E+00	4.7493E+00	1.1567E+01	8.5453E+01	1.9110E+01	4.9856E+01
RPBILDE	1.0774E+01	4.3885E+00	3.7071E+00	3.2265E+00	1.6548E+01	**3.3518E+01**	2.1217E+01	9.4699E+01
DEMO	2.4246E+01	9.8435E+00	5.3978E+00	3.8840E+00	1.2081E+01	7.6839E+01	4.2702E+01	6.1303E+01
MOEA/D	7.0101E+00	6.0826E+00	2.2510E+00	3.6269E+00	1.8266E+01	1.4713E+02	6.4031E+01	6.4186E+02
UPSEMOA	1.0601E+01	1.0136E+01	3.3770E+00	5.1602E+00	1.1556E+01	7.6227E+01	2.8367E+01	6.7166E+01
NSGA-III	3.2208E+01	1.2184E+01	1.3678E+01	4.2531E+01	5.7463E+01	1.0576E+02	4.4318E+02	4.6016E+02
RVEA	1.7147E+02	9.1406E+01	3.3304E+01	4.4978E+09	2.5561E+02	3.4437E+02	6.7471E+02	1.2496E+03
MnKnEA	6.4100E+01	9.7955E+01	3.7923E+00	6.3529E+00	5.7638E+01	8.2303E+01	3.7782E+02	5.6975E+02
MMIPDE	7.4760E+00	4.4598E+00	4.8365E+00	4.1562E+00	1.6377E+01	4.0040E+01	2.8355E+01	**3.7209E+01**

Table 7
Friedman's rank of generational distance obtained from the eighteen algorithms (the bold indicates the best solution).

Friedman's rank of GD	10-bar	25-bar	37-bar	60-bar	72-bar	120-bar	200-bar	942-bar	Overall Friedman's value	Overall Friedman rank
MOALO	14.53	12.17	14.77	6.37	11.37	10.50	12.60	7.73	90.03	13
MODA	13.03	12.30	12.97	10.97	9.47	8.97	12.93	10.10	90.73	14
MOGOA	14.13	13.10	15.30	12.33	12.53	9.00	12.77	12.73	101.90	15
MOGWO	6.50	3.13	**1.27**	15.43	3.33	13.77	**2.03**	4.03	49.50	5
MOMVO	7.37	7.50	4.40	9.13	7.10	9.17	12.17	13.30	70.13	9
MOWCA	4.37	7.80	5.10	9.63	7.80	7.80	5.80	6.93	55.23	6
MSSA	8.83	11.40	10.87	8.90	8.17	11.30	13.23	10.83	83.53	11
SHAMODE	9.13	9.47	9.27	8.60	7.97	9.37	4.87	5.17	63.83	8
SHAMODE-WO	8.33	8.53	8.10	9.10	8.93	9.53	5.00	5.10	62.63	7
NSGA-II	4.87	5.83	4.80	4.13	2.90	3.50	5.77	6.43	38.23	2
RPBILDE	9.43	8.97	11.33	11.07	11.57	10.47	9.23	9.67	81.73	10
DEMO	5.00	5.07	10.70	**1.43**	3.60	**2.87**	5.20	5.53	39.40	3
MOEA/D	**1.53**	**1.63**	2.70	3.63	15.33	3.40	3.97	12.80	45.00	4
UPSEMOA	3.63	3.23	7.77	3.10	**1.67**	3.27	5.07	6.17	**33.90**	**1**
NSGA-III	14.57	13.17	13.60	16.57	13.00	13.37	16.77	16.20	117.23	17
RVEA	17.93	17.53	17.87	17.97	17.77	17.97	17.87	17.87	142.77	18
MnKnEA	16.20	17.00	6.73	12.93	16.33	14.00	16.37	16.53	116.10	16
MMIPDE	11.60	13.17	13.47	9.70	12.17	12.77	9.37	**3.87**	86.10	12

Table 8
Mean inverted generational distance obtained from the eighteen algorithms (the bold indicates the best solution).

Mean IGD	10-bar	25-bar	37-bar	60-bar	72-bar	120-bar	200-bar	942-bar
MOALO	1.4806E+03	6.8123E+02	4.0726E+02	1.9630E+03	1.1247E+03	1.1240E+04	2.0294E+03	2.6903E+04
MODA	1.9255E+03	4.7305E+02	3.5161E+02	1.2993E+03	9.8828E+02	7.4820E+03	2.4706E+03	2.9288E+04
MOGOA	1.6072E+03	5.5153E+02	4.6179E+02	1.5430E+03	1.2034E+03	7.4694E+03	2.4801E+03	3.0877E+04
MOGWO	2.8172E+03	8.9487E+02	5.4139E+02	1.5724E+03	1.4497E+03	1.2723E+04	1.6000E+03	2.2374E+04
MOMVO	1.6829E+03	6.0506E+02	5.1983E+02	1.7362E+03	1.3575E+03	1.4699E+04	2.7172E+03	2.6582E+04
MOWCA	2.6927E+03	1.1003E+03	6.0056E+02	1.8738E+03	1.5021E+03	1.2045E+04	2.2846E+03	2.8915E+04
MSSA	2.2356E+03	8.8947E+02	5.1974E+02	1.6632E+03	1.3337E+03	8.9539E+03	2.5426E+03	3.2877E+04
SHAMODE	**2.1623E+02**	1.5542E+02	1.0102E+02	8.3572E+02	5.7391E+02	2.6856E+03	1.5055E+03	1.4006E+04
SHAMODE-WO	2.3816E+02	1.3304E+02	5.9742E+01	6.1202E+02	3.7066E+02	2.2832E+03	4.9125E+02	4.2276E+03
NSGA-II	6.2535E+02	2.8857E+02	3.3907E+02	1.0375E+03	7.8724E+02	3.0351E+03	1.5541E+03	2.1957E+04
RPBILDE	4.6112E+02	2.1148E+02	2.4192E+02	9.7155E+02	5.9368E+02	3.7877E+03	9.7191E+02	1.7119E+04
DEMO	5.0990E+02	2.2795E+02	1.8146E+02	1.0931E+03	4.3656E+02	2.7457E+03	1.0657E+03	2.0908E+04
MOEA/D	2.4700E+03	5.6256E+02	2.9010E+02	1.4326E+03	7.3300E+02	9.1046E+03	2.4763E+03	1.8657E+04
UPSEMOA	8.4647E+02	3.8176E+02	2.9671E+02	1.2672E+03	9.2230E+02	3.8405E+03	1.2976E+03	2.1356E+04
NSGA-III	2.2665E+03	9.8649E+02	5.4152E+02	1.8109E+03	1.3630E+03	9.5370E+03	3.1080E+03	3.5940E+04
RVEA	1.7440E+03	6.7328E+02	6.3699E+02	2.6667E+09	1.4208E+03	5.6594E+03	3.1604E+03	3.3263E+04
MnKnEA	2.2016E+03	7.6360E+02	3.4608E+02	1.7141E+03	1.2245E+03	5.3009E+03	2.7698E+03	3.3200E+04
MMIPDE	3.3391E+02	**7.6946E+01**	**4.8572E+01**	**1.1536E+02**	**1.6118E+02**	**1.2473E+03**	**4.7512E+02**	**1.3845E+03**

Table 9
Standard deviation of inverted generational distance obtained from the eighteen algorithms (the bold indicates the best solution).

STD of IGD	10-bar	25-bar	37-bar	60-bar	72-bar	120-bar	200-bar	942-bar
MOALO	4.5024E+02	2.0692E+02	8.8295E+01	2.5944E+02	3.4872E+02	2.3563E+03	3.9079E+02	4.5359E+03
MODA	5.5839E+02	1.8637E+02	1.0637E+02	2.3293E+02	2.8050E+02	1.4503E+03	3.2171E+02	2.8183E+03
MOGOA	6.2032E+02	1.8969E+02	9.9508E+01	2.4216E+02	2.2989E+02	2.6143E+03	3.0842E+02	3.0285E+03
MOGWO	2.9454E+02	9.0443E+01	7.4452E+01	2.3610E+02	1.5734E+02	1.6042E+03	6.8806E+02	7.6460E+03
MOMVO	6.7253E+02	2.5327E+02	1.3495E+02	3.0747E+02	2.9567E+02	3.7828E+03	5.6882E+02	3.1849E+03
MOWCA	8.7800E+02	2.8010E+02	1.6139E+02	3.1625E+02	3.2573E+02	2.3345E+03	3.9972E+02	2.8464E+03
MSSA	5.7647E+02	2.4049E+02	9.2814E+01	2.5003E+02	3.5138E+02	2.2285E+03	2.6927E+02	2.8731E+03
SHAMODE	**9.7452E+01**	5.8236E+01	3.2775E+01	1.3049E+02	1.3946E+02	1.0299E+03	3.2223E+02	2.7235E+03
SHAMODE-WO	1.2693E+02	3.8697E+01	2.2325E+01	1.4512E+02	1.2047E+02	7.7296E+02	1.6171E+02	1.3338E+03
NSGA-II	3.0270E+02	1.0797E+02	7.2902E+01	2.3445E+02	1.7766E+02	8.6510E+02	3.1984E+02	3.3215E+03
RPBILDE	3.1224E+02	1.1938E+02	8.6374E+01	1.9441E+02	1.5647E+02	1.5535E+03	1.8108E+02	2.1719E+03
DEMO	1.6066E+02	7.3685E+01	4.6788E+01	1.9351E+02	1.3673E+02	1.0645E+03	2.5239E+02	2.0243E+03
MOEA/D	7.3338E+02	1.8238E+02	6.1920E+01	2.9935E+02	2.5432E+02	2.4556E+03	3.8668E+02	5.1003E+03
UPSEMOA	3.2691E+02	1.2787E+02	6.1834E+01	1.7838E+02	1.9454E+02	1.0970E+03	2.6360E+02	1.9081E+03
NSGA-III	6.0213E+02	2.6356E+02	1.8319E+02	2.5500E+02	2.4636E+02	2.9343E+03	2.9779E+02	2.3882E+03
RVEA	5.8902E+02	2.4681E+02	1.3633E+02	4.4978E+09	4.5441E+02	2.3773E+03	4.9636E+02	2.5856E+03
MnKnEA	5.3476E+02	2.1735E+02	4.6025E+01	1.9827E+02	2.6043E+02	7.5656E+02	3.3484E+02	2.5413E+03
MMIPDE	2.9215E+02	**2.9586E+01**	**1.8824E+01**	**4.5938E+01**	**7.2272E+01**	**5.3460E+02**	**1.2606E+02**	**2.7976E+02**

Table 10
Friedman's rank of inverted generational distance obtained from the eighteen algorithms (the bold indicates the best solution).

Friedman's rank of mean IGD	10-bar	25-bar	37-bar	60-bar	72-bar	120-bar	200-bar	942-bar	Overall Friedman's value	Overall Friedman rank
MOALO	9.87	11.97	11.13	15.73	11.37	14.67	9.33	11.00	95.07	11
MODA	12.30	9.43	9.57	8.33	9.73	11.00	12.63	12.53	85.53	9
MOGOA	10.60	10.03	12.67	11.23	12.00	10.90	12.57	13.50	93.50	10
MOGWO	16.27	15.13	14.90	11.50	15.13	16.17	7.43	8.70	105.23	14
MOMVO	11.00	10.57	13.70	13.17	13.73	16.87	13.77	10.50	103.30	13
MOWCA	15.07	16.33	15.13	14.40	15.17	15.40	11.43	12.20	115.13	17
MSSA	13.70	14.63	14.30	12.33	13.63	12.87	13.30	15.07	109.83	15
SHAMODE	**2.27**	3.27	3.10	3.67	4.87	4.07	6.60	3.70	31.53	3
SHAMODE-WO	2.43	2.73	1.97	2.30	2.63	3.30	**1.50**	2.03	18.90	2
NSGA-II	5.60	6.10	8.90	5.57	7.43	4.50	6.83	7.83	52.77	6
RPBILDE	4.43	4.63	6.13	4.80	5.13	6.20	3.87	4.83	40.03	5
DEMO	4.97	5.27	4.57	5.87	3.37	4.17	4.57	6.80	39.57	4
MOEA/D	14.53	10.87	7.33	9.93	6.43	12.60	12.67	5.80	80.17	8
UPSEMOA	6.87	7.93	7.27	7.90	9.00	6.10	5.67	7.23	57.97	7
NSGA-III	13.60	15.83	13.97	14.07	14.07	13.33	16.57	17.13	118.57	18
RVEA	11.17	12.00	16.17	16.03	13.87	9.07	16.13	15.60	110.03	16
MnKnEA	13.40	13.07	8.93	13.17	12.30	8.53	14.50	15.53	99.43	12
MMIPDE	2.93	**1.20**	**1.27**	**1.00**	**1.13**	**1.27**	1.63	**1.00**	**11.43**	**1**

while SHAMODE obtains the best solutions in 10–bar truss. Table 10 presents Friedman's rank of HV obtained from the eighteen algorithms. It is noticed from the table that MMIPDE obtains the best solutions in 25–bar, 37–bar, 60–bar, 72–bar, 120–bar, and 942–bar trusses; SHAMODE obtains the best solutions in 10–bar truss; SHAMODE–WO obtains the best solutions in 200–bar truss. The overall performance of MMIPDE based on GD results is the best among the evaluated MHs and SHAMODE–WO performs second best.

Table 11 presents mean STE obtained from the eighteen algorithms. It is noticed from the table that MMIPDE outperforms the others. Table 12 presents STD of STE obtained from the eighteen algorithms. It is noticed from the table that MMIPDE obtains the best solutions in 25–bar, 37–bar, 60–bar, 72–bar, 120–bar, 200–bar, 942–bar trusses while RPBILDE obtains the best solutions in 10–bar truss. Table 13 presents Friedman's rank of STE obtained from the eighteen algorithms. It is noticed from the table that MMIPDE outperforms the others. The overall performance of MMIPDE based on STE results is the best among the evaluated MHs and MOGOA performs second best.

From the result tables, the effectiveness of the MHs in MO truss problems are evaluated by considering several characteristics with the use of the HV, GD, IGD, and STE metrics. The HV values in most of the truss problems coincide with the IGD & STE results. MMIPDE provides the best results in HV, IGD & STE. SHAMODE–WO is ranked second among the evaluated algorithms in HV, IGD & STE. The results of GD are slightly different from the results of HV, IGD, & STE. One of the reasons for this slight difference in GD results could be due to the measurement technique of GD. GD is the only measure of Euclidian distances of the received front to the reference front. The GD can represent the advancement of the front, but it cannot capture the spread of obtained front. However, IGD and HV are measures of both the improvement and the spread of PF. STE is a measure of the front extension and distribution. Thus, HV, IGD, and STE are more reliable than GD.

Table 11
Mean Spacing-to-Extent obtained from the eighteen algorithms (the bold indicates the best solution).

Mean STE	10-bar	25-bar	37-bar	60-bar	72-bar	120-bar	200-bar	942-bar
MOALO	1.4058E-02	2.1080E-02	1.7401E-02	1.8399E-02	2.0177E-02	1.9598E-02	1.7906E-02	1.9971E-02
MODA	2.3243E-02	2.4375E-02	2.2079E-02	2.1627E-02	2.4601E-02	1.8621E-02	2.2207E-02	2.1171E-02
MOGOA	1.0381E-02	1.2630E-02	1.1341E-02	9.4110E-03	1.4590E-02	1.2773E-02	8.8150E-03	9.1448E-03
MOGWO	1.6228E-02	1.5713E-02	1.3308E-02	1.4800E-02	1.4586E-02	1.5969E-02	1.4629E-02	1.7575E-02
MOMVO	1.4652E-02	1.6420E-02	1.3152E-02	1.2723E-02	1.6297E-02	1.4224E-02	1.7311E-02	1.1643E-02
MOWCA	2.4132E-02	2.4000E-02	2.0847E-02	1.9541E-02	1.9535E-02	2.0824E-02	1.4541E-02	1.2231E-02
MSSA	1.7990E-02	2.1458E-02	1.7520E-02	1.4835E-02	2.0780E-02	1.7066E-02	1.7266E-02	1.3334E-02
SHAMODE	9.5951E-03	1.3958E-02	1.0188E-02	9.9350E-03	1.5642E-02	1.2517E-02	1.2496E-02	8.8132E-03
SHAMODE-WO	9.2807E-03	1.3021E-02	9.8230E-03	1.0103E-02	1.3942E-02	1.1675E-02	1.2223E-02	1.1272E-02
NSGA-II	1.2715E-02	1.6419E-02	1.4639E-02	9.3584E-03	1.4049E-02	1.2980E-02	9.9082E-03	8.7090E-03
RPBILDE	9.6989E-03	1.3033E-02	1.0597E-02	9.5702E-03	1.4798E-02	1.2437E-02	1.2219E-02	9.1043E-03
DEMO	1.7599E-02	1.7219E-02	1.6111E-02	1.9296E-02	1.5868E-02	2.0102E-02	1.0719E-02	7.8853E-03
MOEA/D	3.2216E-02	2.3162E-02	1.6997E-02	2.5761E-02	1.3407E-02	2.3888E-02	2.4670E-02	2.0502E-02
UPSEMOA	1.5691E-02	1.7495E-02	1.4894E-02	1.8478E-02	2.0276E-02	1.6335E-02	1.2004E-02	8.8472E-03
NSGA-III	1.7752E-02	1.7630E-02	1.6782E-02	2.2849E-02	1.8651E-02	1.4456E-02	2.2267E-02	2.4113E-02
RVEA	5.0073E-02	5.7258E-02	5.4782E-02	1.6667E+19	5.8759E-02	3.3767E-02	1.2123E-01	6.2778E-02
MnKnEA	1.6605E-02	2.9215E-02	1.3429E-02	1.1767E-02	2.7206E-02	1.3210E-02	3.1419E-02	3.2306E-02
MMIPDE	**6.4144E-03**	**5.5889E-03**	**4.9649E-03**	**3.1946E-03**	**6.7002E-03**	**4.2986E-03**	**4.3482E-03**	**2.3605E-03**

Table 12
Standard deviation of Spacing-to-Extent obtained from the eighteen algorithms (the bold indicates the best solution).

STD of STE	10-bar	25-bar	37-bar	60-bar	72-bar	120-bar	200-bar	942-bar
MOALO	3.3561E-03	6.9284E-03	5.5463E-03	6.6084E-03	3.3218E-03	6.1488E-03	4.7779E-03	6.8412E-03
MODA	1.0061E-02	6.9392E-03	7.9053E-03	9.1518E-03	5.4421E-03	5.1437E-03	6.9953E-03	1.0864E-02
MOGOA	3.7068E-03	3.6893E-03	3.9860E-03	3.2873E-03	5.2068E-03	3.8012E-03	3.6974E-03	7.4588E-03
MOGWO	7.6182E-03	4.7067E-03	5.5221E-03	5.9783E-03	4.2892E-03	4.8662E-03	5.7617E-03	7.8930E-03
MOMVO	5.3913E-03	6.7759E-03	5.6714E-03	5.4805E-03	3.8567E-03	5.4288E-03	6.8637E-03	5.3433E-03
MOWCA	1.1528E-02	1.1618E-02	9.7556E-03	8.7482E-03	5.9482E-03	1.0748E-02	4.9980E-03	4.9278E-03
MSSA	9.0717E-03	1.0451E-02	1.0323E-02	8.4406E-03	7.4219E-03	8.1412E-03	6.6403E-03	7.7244E-03
SHAMODE	3.0743E-03	3.0917E-03	2.3670E-03	2.2144E-03	2.9143E-03	2.5108E-03	2.8246E-03	3.0601E-03
SHAMODE-WO	3.6444E-03	2.1185E-03	2.1181E-03	3.3575E-03	1.9177E-03	1.5730E-03	2.4400E-03	3.4165E-03
NSGA-II	6.6176E-03	4.8043E-03	5.8719E-03	3.3032E-03	4.1057E-03	2.8501E-03	2.9708E-03	3.0054E-03
RPBILDE	**2.9431E-03**	2.7120E-03	1.8721E-03	2.5908E-03	3.1043E-03	2.3593E-03	3.1997E-03	3.8551E-03
DEMO	7.0534E-03	5.0320E-03	8.2268E-03	1.1696E-02	4.1489E-03	8.8074E-03	4.0236E-03	2.7173E-03
MOEA/D	1.3037E-02	6.4157E-03	6.1683E-03	1.1885E-02	4.2613E-03	8.0479E-03	1.3341E-02	1.5232E-02
UPSEMOA	8.2042E-03	4.2306E-03	5.1610E-03	9.1233E-03	7.6190E-03	5.0682E-03	2.8482E-03	2.4004E-03
NSGA-III	9.8004E-03	5.6975E-03	1.2166E-02	1.6785E-02	7.5630E-03	4.8560E-03	1.3048E-02	3.6745E-02
RVEA	2.6529E-02	3.0642E-02	3.4046E-02	3.7905E+19	4.2468E-02	9.9614E-03	7.5706E-02	3.8779E-02
MnKnEA	1.5634E-02	2.8796E-02	4.1163E-03	4.7013E-03	9.5645E-03	2.9926E-03	1.2103E-02	1.2361E-02
MMIPDE	3.4406E-03	**1.0526E-03**	**1.4025E-03**	**5.9727E-04**	**1.6658E-03**	**6.4999E-04**	**8.2324E-04**	**2.2664E-04**

Table 13
Friedman's rank of Spacing-to-Extent obtained from the eighteen algorithms (the bold indicates the best solution).

Friedman's rank of mean STE	10-bar	25-bar	37-bar	60-bar	72-bar	120-bar	200-bar	942-bar	Overall Friedman's value	Overall Friedman rank
MOALO	9.90	12.20	12.13	12.47	12.40	13.07	12.17	13.47	97.80	15
MODA	13.43	13.90	14.00	13.40	14.83	12.30	13.57	13.40	108.83	17
MOGOA	6.53	5.17	7.03	5.87	6.90	6.97	4.17	5.90	48.53	2
MOGWO	9.70	8.50	8.27	10.03	7.37	10.03	9.20	12.17	75.27	9
MOMVO	9.43	8.50	8.50	8.47	8.57	8.13	10.97	8.70	71.27	7
MOWCA	13.07	12.27	13.40	12.93	11.37	11.90	9.50	9.33	93.77	14
MSSA	10.63	11.33	11.10	9.67	11.67	9.63	11.10	9.60	84.73	12
SHAMODE	5.37	6.60	5.50	5.90	8.27	7.03	7.80	6.47	52.93	5
SHAMODE-WO	4.77	5.87	5.10	5.57	6.17	5.67	7.37	9.00	49.50	3
NSGA-II	7.47	8.73	9.67	5.13	6.43	7.17	4.80	6.17	55.57	6
RPBILDE	5.47	5.90	6.13	5.37	7.67	6.67	7.70	6.60	51.50	4
DEMO	11.20	9.30	10.23	11.43	8.33	12.70	5.67	5.33	74.20	8
MOEA/D	15.43	13.17	11.90	14.63	6.00	14.47	13.30	12.63	101.53	16
UPSEMOA	9.90	10.10	10.50	11.87	11.37	10.63	7.40	6.63	78.40	10
NSGA-III	10.37	9.60	9.50	12.07	10.30	8.80	11.90	11.43	83.97	11
RVEA	17.13	17.03	17.80	17.43	17.30	17.23	17.67	17.33	138.93	18
MnKnEA	8.80	11.63	9.03	7.73	14.93	7.57	15.63	15.80	91.13	13
MMIPDE	**2.40**	**1.20**	**1.20**	**1.03**	**1.13**	**1.03**	**1.10**	**1.03**	**10.13**	**1**

Table 14
Average Friedman's rank from all indicators obtained from the eighteen algorithms (the bold indicates the best solution)

Average Friedman's rank	10-bar	25-bar	37-bar	60-bar	72-bar	120-bar	200-bar	942-bar	Overall Friedman's value	Overall Friedman rank
MOALO	11.92	12.46	12.78	12.83	12.54	13.41	12.28	12.25	100.45	15
MODA	13.01	11.34	12.17	11.53	11.32	10.95	13.26	12.59	96.17	14
MOGOA	10.57	10.00	11.98	10.83	10.73	9.98	10.71	11.14	85.94	11
MOGWO	11.38	10.41	10.11	12.71	9.53	13.94	6.71	7.67	82.45	10
MOMVO	8.61	8.35	8.70	9.39	8.88	11.37	10.67	9.32	75.28	8
MOWCA	11.02	12.16	11.38	11.83	10.76	11.34	9.18	9.73	87.39	12
MSSA	11.38	12.93	12.57	10.79	11.10	12.13	12.56	12.30	95.76	13
SHAMODE	4.74	5.47s	5.08	5.27	6.10	5.77	5.71	5.28	43.41	3
SHAMODE-WO	**4.53**	5.03	4.50	4.94	5.05	5.33	4.03	4.68	38.08	2
NSGA-II	6.34	6.88	7.71	5.62	6.84	5.93	6.58	7.85	53.73	5
RPBILDE	5.73	5.75	6.73	6.09	6.86	6.74	5.88	5.68	49.47	4
DEMO	7.17	6.87	8.07	7.17	6.12	7.28	5.96	6.55	55.17	6
MOEA/D	11.18	9.30	8.80	10.03	9.78	11.53	9.22	9.73	79.56	9
UPSEMOA	6.81	7.50	7.87	7.27	7.61	6.98	6.53	6.72	57.28	7
NSGA_III	12.41	12.48	12.81	13.98	12.31	10.91	15.06	14.50	104.46	17
RVEA	15.64	15.76	17.30	17.34	16.63	14.63	17.24	16.75	131.28	18
MnKnEA	13.93	14.18	8.13	10.16	14.93	8.77	15.85	16.01	101.95	16
MMIPDE	4.66	**4.15**	**4.33**	**3.23**	**3.93**	**4.04**	**3.59**	**2.26**	**30.18**	**1**

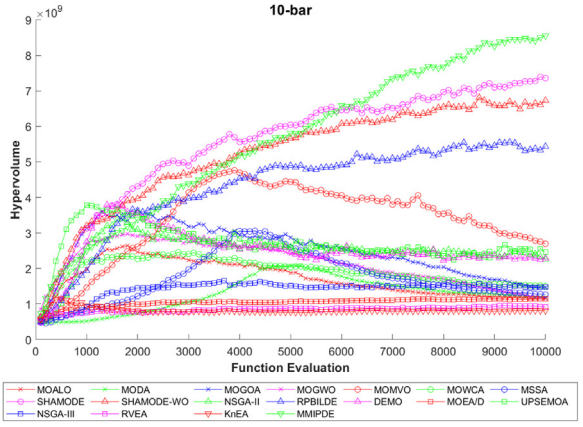

Fig. 5. Mean HV Vs Iteration of the 10-bar tower truss.

To measure the overall performance comparison among the eighteen algorithms, the average mean Friedman's rank of all the evaluated algorithms is calculated and presented in Table 14. The overall best performer as per the average Friedman rank is MMIPDE while SHAMODE–WO and SHAMODE are the runners-up. MMIPDE reported the best average Friedman's ranks in 7 out of 8 truss designs.

Figs. 5-12 present the convergence history of mean HV of the evaluated algorithms for the eight truss problems. Convergence history illustrates that there are nearly four algorithms that perform better compared to others in all the evaluated problems. MMIPDE, SHAMODE, SHAMODE–WO, and RPBILDE have reported good consistency and convergence rate. The remaining algorithms perform somewhat unreliable and reported lower values of mean HV for the evaluated problems. These comprise MOALO, MODA, MOGOA, MOGWO, MOMVO, MOWCA, MSSA, NSGA–II, DEMO, MOEA/D, UPSEMOA, NSGA–III, and MnKnEA while RVEA is at the bottom. MMIPDE seems to be a better performer across with low design to a higher number of design variables while SHAMODE–WO and RPBILDE perform better compared to others in large–scale problems like the 942–bar and 200–bar trusses. SHAMODE–WO reported the second–best performer, but its performance improved while designing a large–scale problems. Overall, the results of MMIPDE show that MMIPDE is the most efficient MHs for designing many-objective optimisation of truss problems while the SHAMODE-WO and SHAMODE are subsequent performers. MMIPDE exploits an estimation of distribution algorithm (EDA) for assigning the control parameters during an optimization run while its reproduction is modified from the traditional DE. This implies that algorithm self-adaptation by means of EDA is efficient for many-objective truss design. The comparative results from this paper are the most updated baseline results for truss many-objctive design as more newly published algorithms have been added to the comparison. Nevertheless, although some top performers have been found out, it hardly implies that such powerful algorithms will always be powerful for other optimization problems. This is often referred to as the no-free-lunch theory stating that one algorithm that is powerful for one particular problem is not always efficient for other optimization problems.

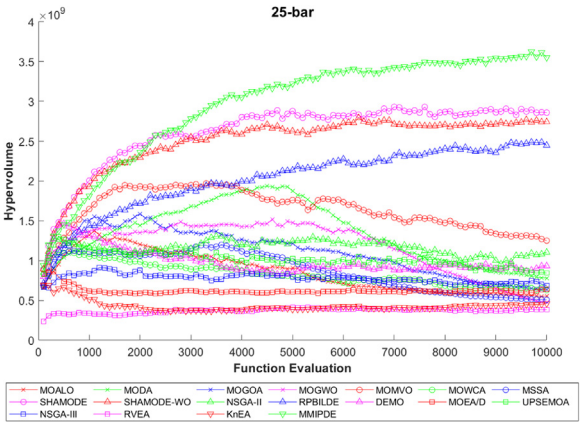

Fig. 6. Mean HV Vs Iteration of the 25-bar tower truss.

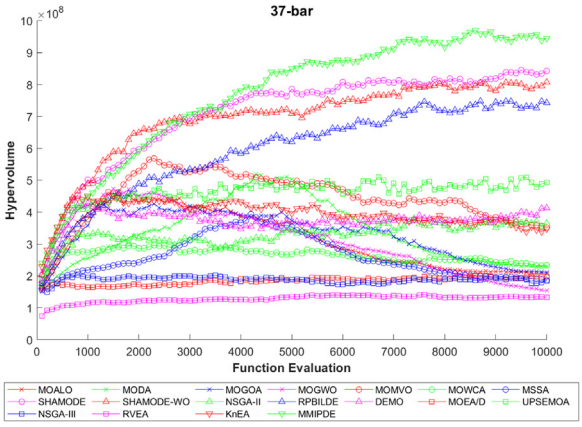

Fig. 7. Mean HV Vs Iteration of the 37-bar tower truss.

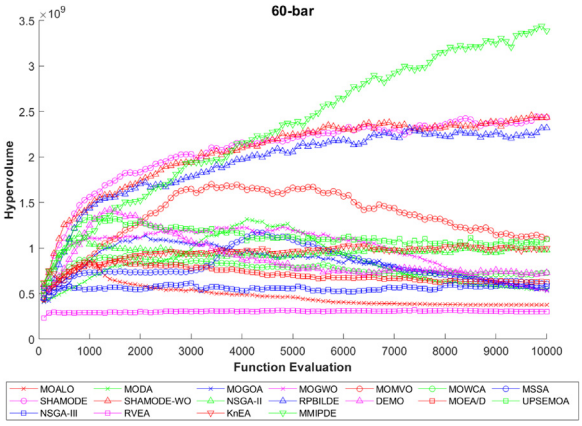

Fig. 8. Mean HV Vs Iteration of the 60-bar tower truss.

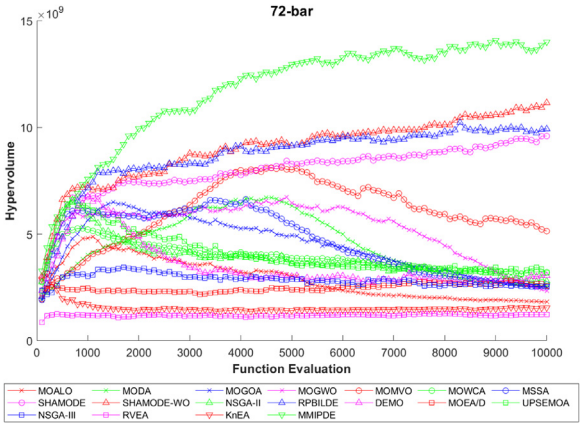

Fig. 9. Mean HV Vs Iteration of the 72-bar tower truss.

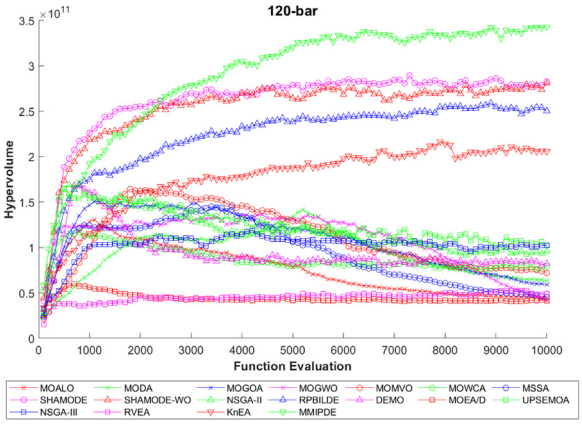

Fig. 10. Mean HV Vs Iteration of the 120-bar tower truss.

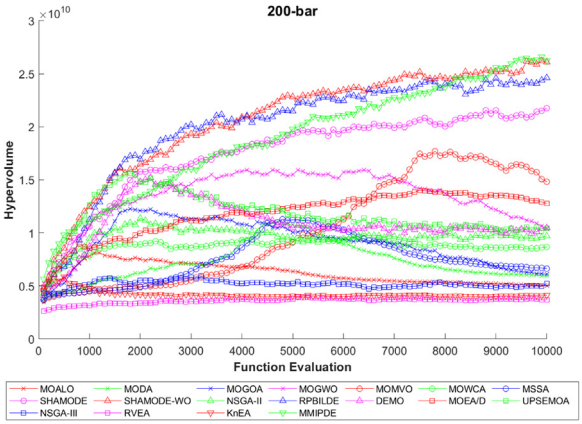

Fig. 11. Mean HV Vs Iteration of the 200-bar tower truss.

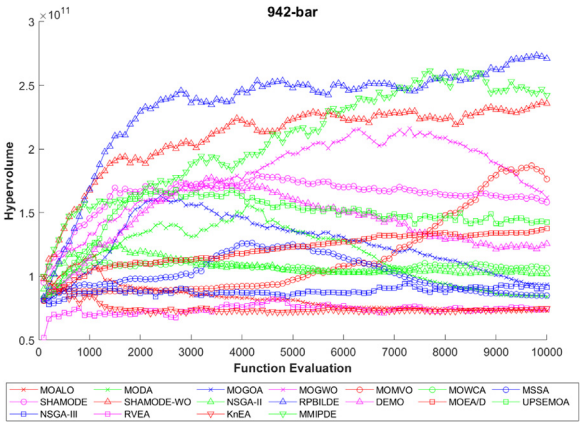

Fig. 12. Mean HV Vs Iteration of the 942-bar tower truss.

Conclusions

Design optimization for real-world structures poses many conflicting objectives and has numerous design constraints, making it a challenging task that requires significant effort to resolve. It is crucial to assess the performance of contemporary algorithms on many-objective truss optimization problems, as there are limited optimization methods available for solving them, to create more efficient methods in the future. Therefore this study compared the performance of new and established multi-objective meta-heuristics to design many-objective trusses. Eight challenging trusses, mostly tested in literature, are modified and used to set up the many-objective test problems. The optimization problems aim to find elemental cross-section areas that minimize mass, minimize maximum compliance, maximize first natural frequency, and minimize maximum buckling factor, subject to elemental stress constraints and buckling constraints. The MOALO, MODA, MOGOA, MOGWO, MOMVO, MOWCA, MSSA, SHAMODE, SHAMODE-WO, NSGA-II, RPBILDE, DEMO, MOEA/D, UPSEMOA, NSGA-III, RVEA, MnKnEA, and MMIPDE algorithms are compared using HV, GD, IGD, and STE measures. Friedman's rank test is performed to get a statistical measure of the eighteen different algorithms. The comparative results, based on the performance measures, reveal that MMIPDE is the overall best performer while SHAMODE-WO and SHAMODE are the second and third best performers, respectively.

Ethics statements

Hereby, we assure that for the manuscript /insert title/ the following is fulfilled:

1) *This material is the authors' own original work, which has not been previously published elsewhere.*
2) *The paper is not currently being considered for publication elsewhere.*
3) *The paper reflects the authors' own research and analysis in a truthful and complete manner.*
4) *The paper properly credits the meaningful contributions of co-authors and co-researchers.*
5) *The results are appropriately placed in the context of prior and existing research.*
6) *All sources used are properly disclosed (correct citation). Literally copying of text must be indicated as such by using quotation marks and giving proper reference.*
7) *All authors have been personally and actively involved in substantial work leading to the paper, and will take public responsibility for its content.*

Declaration of Competing Interests

The authors declare that they have no known competing financial interests or personal relationships that could have appeared to influence the work reported in this paper.

CRediT authorship contribution statement

Natee Panagant: Conceptualization, Methodology, Software, Formal analysis, Data curation, Writing – original draft, Writing – review & editing. **Sumit Kumar:** Conceptualization, Methodology, Formal analysis, Writing – original draft, Writing – review & editing. **Ghanshyam G. Tejani:** Conceptualization, Methodology, Software, Formal analysis, Data curation, Writing – original draft, Writing – review & editing, Supervision, Project administration. **Nantiwat Pholdee:** Conceptualization, Methodology, Software, Formal analysis, Data curation, Writing – original draft, Writing – review & editing, Supervision, Project administration. **Sujin Bureerat:** Funding acquisition, Conceptualization, Methodology, Software, Formal analysis, Data curation, Writing – original draft, Writing – review & editing, Supervision, Project administration.

Data availability

Data will be made available on request.

Acknowledgments

The authors are grateful for the support from the National Research Council Thailand (Grant No. N42A650549).

References

[1] P. Pachung, J.C. Bansal, An improved tangent search algorithm, MethodsX 9 (2022) 101839, doi:10.1016/j.mex.2022.101839.
[2] J.A. Stampfli, D.G. Olsen, B. Wellig, R. Hofmann, A parallelized hybrid genetic algorithm with differential evolution for heat exchanger network retrofit, MethodsX 9 (2022) 101711, doi:10.1016/J.MEX.2022.101711.
[3] S. Kumar, G.G. Tejani, N. Pholdee, S. Bureerat, Multi-Objective Passing Vehicle Search algorithm for structure optimization, Expert Syst. Appl. 169 (2021) 114511.
[4] S. Kumar, G.G. Tejani, N. Pholdee, S. Bureerat, P. Mehta, Hybrid Heat Transfer Search and Passing Vehicle Search optimizer for multi-objective structural optimization, Knowledge-Based Systems 212 (2021) 106556.
[5] M.H. Nguyen, V.P. La, T.T. Le, Q.H. Vuong, Introduction to Bayesian Mindsponge Framework analytics: An innovative method for social and psychological research, MethodsX 9 (2022) 101808, doi:10.1016/j.mex.2022.101808.
[6] S. Kumar, G.G. Tejani, N. Pholdee, S. Bureerat, Multiobjecitve structural optimization using improved heat transfer search, Knowledge-Based Systems 219 (2021) 106811.
[7] S. Kumar, G.G. Tejani, N. Pholdee, S. Bureerat, Multi-objective modified heat transfer search for truss optimization, Eng. Comput. (2020) 1–16.
[8] D.C. Manheim, R.L. Detwiler, Accurate and reliable estimation of kinetic parameters for environmental engineering applications: A global, multi objective, Bayesian optimization approach, MethodsX 6 (2019) 1398–1414, doi:10.1016/j.mex.2019.05.035.
[9] B.A. Ndiogou, A. Thiam, C. Mbow, et al., Modeling and optimization method of an indirectly irradiated solar receiver, MethodsX 6 (2019) 43–55, doi:10.1016/j.mex.2018.12.006.
[10] R.J. Lygoe, M. Cary, P.J. Fleming, A real-world application of a many-objective optimisation complexity reduction process, in: International Conference on Evolutionary Multi-Criterion Optimization, Springer, Berlin, Heidelberg, 2013, pp. 641–655.
[11] G. Fu, Z. Kapelan, J.R. Kasprzyk, P. Reed, Optimal design of water distribution systems using many-objective visual analytics, J. Water Resour. Plann. Manage. 139 (6) (2013) 624–633.
[12] J.G. Herrero, A. Berlanga, J.M.M. López, Effective evolutionary algorithms for many-specifications attainment: Application to air traffic control tracking filters, IEEE Trans. Evol. Comput. 13 (1) (2008) 151–168.
[13] W.J. Xu, L.J. He, G.Y. Zhu, Many-objective flow shop scheduling optimisation with genetic algorithm based on fuzzy sets, Int. J. Prod. Res. 59 (3) (2021) 702–726.
[14] N. Pholdee, S. Bureerat, P. Jaroenapibal, T. Radpukdee, Many-objective optimisation of trusses through meta-heuristics, in: International Symposium on Neural Networks, Springer, Cham, 2017, pp. 143–152.
[15] O. Chikumbo, E. Goodman, K. Deb, Approximating a multi-dimensional Pareto front for a land use management problem: A modified MOEA with an epigenetic silencing metaphor, in: 2012 IEEE congress on evolutionary computation, IEEE, 2012, pp. 1–9.
[16] K. Deb, A. Pratap, S. Agarwal, T.A.M.T. Meyarivan, A fast and elitist multiobjective genetic algorithm: NSGA-II, IEEE Trans. Evol. Comput. 6 (2) (2002) 182–197.
[17] E. Zitzler, M. Laumanns, L. Thiele, SPEA2: Improving the strength Pareto evolutionary algorithm, TIK-report (2001) 103.
[18] H. Ishibuchi, N. Tsukamoto, Y. Nojima, Evolutionary many-objective optimization: A short review, in: 2008 IEEE Congress on Evolutionary Computation (IEEE World Congress on Computational Intelligence), IEEE, 2008, pp. 2419–2426.
[19] K. Li, K. Deb, Q. Zhang, S. Kwong, An evolutionary many-objective optimization algorithm based on dominance and decomposition, IEEE Trans. Evol. Comput. 19 (5) (2014) 694–716.
[20] H. Wang, L. Jiao, X. Yao, Two_Arch2: An improved two-archive algorithm for many-objective optimization, IEEE Trans. Evol. Comput. 19 (4) (2014) 524–541.
[21] M. Li, J. Zheng, R. Shen, K. Li, Q. Yuan, A grid-based fitness strategy for evolutionary many-objective optimization, in: Proceedings of the 12th Annual Conference On Genetic And Evolutionary Computation, 2010, pp. 463–470.
[22] X. Zhang, Y. Tian, Y. Jin, A knee point-driven evolutionary algorithm for many-objective optimization, IEEE Trans. Evol. Comput. 19 (6) (2014) 761–776.
[23] R. Cheng, Y. Jin, M. Olhofer, B. Sendhoff, A reference vector guided evolutionary algorithm for many-objective optimization, IEEE Trans. Evol. Comput. 20 (5) (2016) 773–791.
[24] R. Wang, R.C. Purshouse, P.J. Fleming, Preference-inspired coevolutionary algorithms for many-objective optimization, IEEE Trans. Evol. Comput. 17 (4) (2012) 474–494.
[25] K. Deb, D.K. Saxena, On finding pareto-optimal solutions through dimensionality reduction for certain large-dimensional multi-objective optimization problems, Kangal Report 2005011 (2005) 1–19.
[26] D. Brockhoff, E. Zitzler, Improving hypervolume-based multiobjective evolutionary algorithms by using objective reduction methods, in: 2007 IEEE congress on evolutionary computation, IEEE, 2007, pp. 2086–2093.
[27] H.L. Liu, F. Gu, Q. Zhang, Decomposition of a multiobjective optimization problem into a number of simple multiobjective subproblems, IEEE Trans. Evol. Comput. 18 (3) (2013) 450–455.
[28] K. Deb, H. Jain, An evolutionary many-objective optimization algorithm using reference-point-based nondominated sorting approach, part I: solving problems with box constraints, IEEE Trans. Evol. Comput. 18 (4) (2013) 577–601.
[29] G.G. Tejani, V.J. Savsani, V.K. Patel, Adaptive symbiotic organisms search (SOS) algorithm for structural design optimization, J. Computat. Design Eng. 3 (3) (2016) 226–249.
[30] S. Kumar, G.G. Tejani, S. Mirjalili, Modified symbiotic organisms search for structural optimization, Eng. Comput. 35 (4) (2019) 1269–1296.
[31] G.G. Tejani, V.J. Savsani, V.K. Patel, & S. Mirjalili, Truss optimization with natural frequency bounds using improved symbiotic organisms search, Knowledge-Based Syst. 143 (2018) 162–178.
[32] S. Kumar, G.G. Tejani, N. Pholdee, S. Bureerat, Improved metaheuristics through migration-based search and an acceptance probability for truss optimization, Asian J. Civil Eng. 21 (7) (2020) 1217–1237.
[33] A. Frija, H. Ouerghemmi, F. Ismail, et al., Generic algorithm for multicriteria ranking of crop technological options based on the “Technique for Order of Preference by Similarity to Ideal Solution” using ShinyApps, MethodsX 8 (2021) 101519, doi:10.1016/j.mex.2021.101519.
[34] J.E. Lou, L.F. Larson, S.M. Han, et al., Developing a novel computer visualization system to simulate the uranium upward transport mechanism: Uranium pollution in arid landscapes, MethodsX 9 (2022) 101794, doi:10.1016/j.mex.2022.101794.
[35] V. Savsani, M.A. Tawhid, Non-dominated sorting moth flame optimization (NS-MFO) for multi-objective problems, Eng. Appl. Artif. Intell. 63 (2017) 20–32, doi:10.1016/j.engappai.2017.04.018.
[36] G.G. Tejani, S. Kumar, A.H. Gandomi, Multi-objective heat transfer search algorithm for truss optimization, Eng. Comput. 37 (1) (2021) 641–662.
[37] C.A. Coello, A.D. Christiansen, Multiobjective optimization of trusses using genetic algorithms, Comput. Struct. 75 (6) (2000) 647–660.
[38] R. Peirovi Minaee, M. Afsharnia, A. Moghaddam, et al., Calibration of water quality model for distribution networks using genetic algorithm, particle swarm optimization, and hybrid methods, MethodsX 6 (2019) 540–548, doi:10.1016/J.MEX.2019.03.008.
[39] G.C. Luh, C.H. Chueh, Multi-objective optimal design of truss structure with immune algorithm, Comput. Struct. 82 (11-12) (2004) 829–844.

[40] G.G. Tejani, N. Pholdee, S. Bureerat, D. Prayogo, Multiobjective adaptive symbiotic organisms search for truss optimization problems, Knowl.-based Syst. 161 (2018) 398–414.
[41] S. Kumar, P. Jangir, G.G. Tejani, M. Premkumar, H.H. Alhelou, MOPGO: a new physics-based multi-objective plasma generation optimizer for solving structural optimization problems, IEEE Access, 2021.
[42] S. Gholizadeh, A. Baghchevan, Multi-objective seismic design optimization of steel frames by a chaotic meta-heuristic algorithm, Eng. Comput. 33 (2017) 1045–1060, doi:10.1007/s00366-017-0515-0.
[43] S. Santos CE da, S. Coelho L dos, C.H. Llanos, Nature inspired optimization tools for SVMs - NIOTS, MethodsX 8 (2021) 101574, doi:10.1016/j.mex.2021.101574.
[44] Robati FN, Akbarifard H, Jalaee S abdolmajid (2020) Poverty modeling in the Islamic Republic of Iran using an ANFIS optimized network with the differential evolution algorithm (ANFIS_DE). MethodsX 7:101120. doi:10.1016/j.mex.2020.101120.
[45] J.P.G. Carvalho, É.C. Carvalho, D.E. Vargas, P.H. Hallak, B.S. Lima, A.C. Lemonge, Multi-objective optimum design of truss structures using differential evolution algorithms, Comput. Struct. 252 (2021) 106544.
[46] V. Mokarram, M.R. Banan, A new PSO-based algorithm for multi-objective optimization with continuous and discrete design variables, Struct. Multidiscip. Optim. 57 (2) (2018) 509–533.
[47] S. Mirjalili, P. Jangir, S. Saremi, Multi-objective ant lion optimizer: a multi-objective optimization algorithm for solving engineering problems, Appl. Intell. 46 (1) (2017) 79–95.
[48] S. Mirjalili, Dragonfly algorithm: a new meta-heuristic optimization technique for solving single-objective, discrete, and multi-objective problems, Neural Comput. Appl. 27 (4) (2016) 1053–1073.
[49] S.Z. Mirjalili, S. Mirjalili, S. Saremi, H. Faris, I. Aljarah, Grasshopper optimization algorithm for multi-objective optimization problems, Appl. Intell. 48 (4) (2018) 805–820.
[50] S. Mirjalili, S. Saremi, S.M. Mirjalili, L.D.S. Coelho, Multi-objective grey wolf optimizer: a novel algorithm for multi-criterion optimization, Expert Syst. Appl. 47 (2016) 106–119.
[51] S. Mirjalili, P. Jangir, S.Z. Mirjalili, S. Saremi, I.N. Trivedi, Optimization of problems with multiple objectives using the multi-verse optimization algorithm, Knowledge-Based Systems 134 (2017) 50–71.
[52] A. Sadollah, H. Eskandar, J.H. Kim, Water cycle algorithm for solving constrained multi-objective optimization problems, Appl. Soft Comput. 27 (2015) 279–298.
[53] S. Mirjalili, A.H. Gandomi, S.Z. Mirjalili, S. Saremi, H. Faris, S.M. Mirjalili, Salp Swarm algorithm: a bio-inspired optimizer for engineering design problems, Adv. Eng. Software 114 (2017) 163–191.
[54] N. Panagant, S. Bureerat, K. Tai, A novel self-adaptive hybrid multi-objective meta-heuristic for reliability design of trusses with simultaneous topology, shape and sizing optimisation design variables, Struct. Multidiscip. Optim. 60 (5) (2019) 1937–1955.
[55] N. Pholdee, S. Bureerat, Hybridisation of real-code population-based incremental learning and differential evolution for multiobjective design of trusses, Inf. Sci. 223 (2013) 136–152.
[56] T. Robič, B. Filipič, Differential evolution for multiobjective optimization, in: International Conference On Evolutionary Multi-Criterion Optimization, Springer, Berlin, Heidelberg, 2005, pp. 520–533.
[57] Q. Zhang, H. Li, MOEA/D: a multiobjective evolutionary algorithm based on decomposition, IEEE Trans. Evol. Comput. 11 (6) (2007) 712–731.
[58] T. Aittokoski, K. Miettinen, Efficient evolutionary approach to approximate the Pareto-optimal set in multiobjective optimization, UPS-EMOA, Optimisation Methods Software 25 (6) (2010) 841–858.
[59] K. Deb, A. Pratap, T. Meyarivan, Constrained test problems for multi-objective evolutionary optimization, in: International Conference on Evolutionary Multi--Criterion Optimization. Lecture Notes in computer Science, 2001, pp. 284–298. 1993.